

Hidden Order in a Perovskite Iridate Revealed by Nonlinear Optics

David Hsieh

Institute for Quantum Information and Matter
Department of Physics, Caltech

*KITP Program: New Phases and Emergent Phenomena in Correlated
Materials with Strong Spin-Orbit Coupling*

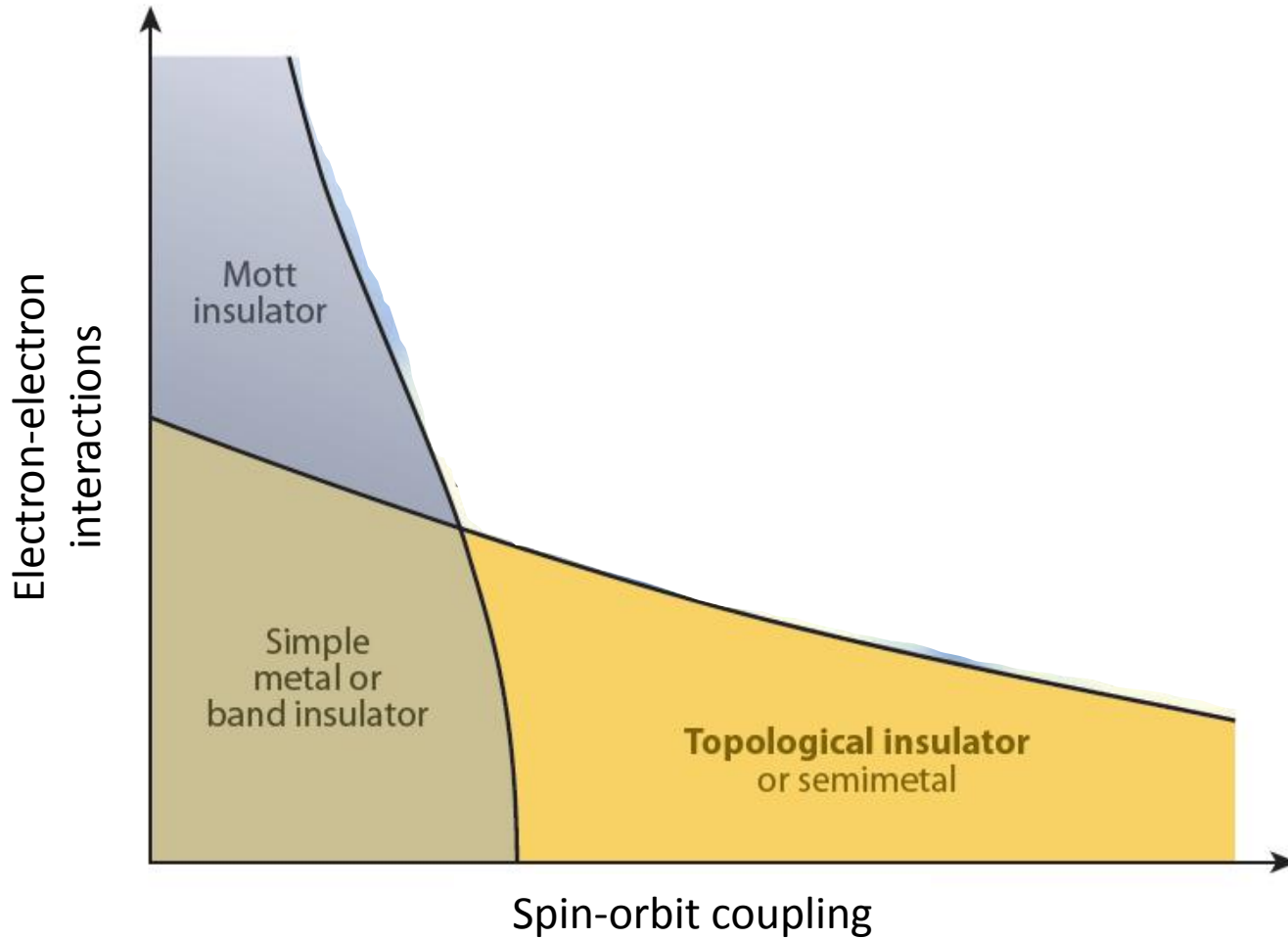
9/15/2015

Caltech

IQIM



Electron correlations + spin-orbit coupling




Outline

- Sr_2IrO_4 : A spin-orbit coupled Mott insulator
- Nonlinear optical harmonic generation
 - A tool for detecting electronic symmetry breaking
 - Principles of operation
 - High precision rotational anisotropy
- Physics of Sr_2IrO_4 revealed through nonlinear optics
 - Perfect magneto-elastic locking via structural distortion
 - A hidden odd-parity magnetic order

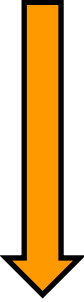
5d transition metal oxides

U



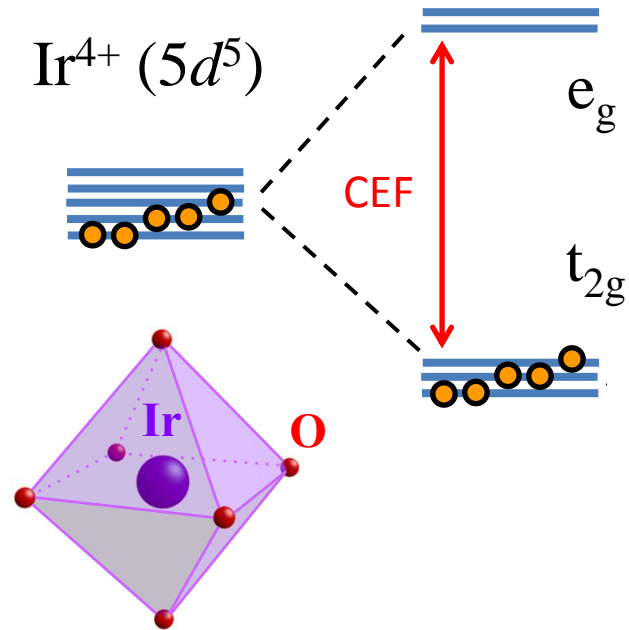
1 H	2 He											13 B	14 C	15 N	16 O	17 F	18 Ne
3 Li	4 Be											5 B	6 C	7 N	8 O	9 F	10 Ne
11 Na	12 Mg											13 Al	14 Si	15 P	16 S	17 Cl	18 Ar
19 K	20 Ca	21 Sc	22 Ti	23 V	24 Cr	25 Mn	26 Fe	27 Co	28 Ni	29 Cu	30 Zn	31 Ga	32 Ge	33 As	34 Se	35 Br	36 Kr
37 Rb	38 Sr	39 Y	40 Zr	41 Nb	42 Mo	43 Tc	44 Ru	45 Rh	46 Pd	47 Ag	48 Cd	49 In	50 Sn	51 Sb	52 Te	53 I	54 Xe
55 Cs	56 Ba	57 La	72 Hf	73 Ta	74 W	75 Re	76 Os	77 Ir	78 Pt	79 Au	80 Hg	81 Tl	82 Pb	83 Bi	84 Po	85 At	86 Rn
87 Fr	88 Ra	89 Ac	104 Rf	105 Db	106 Sg	107 Bh	108 Hs	109 Mt	110 Ds	111 Rg	112 Uub	113 Uut	114 Uuq	115 Uup			

SOC,
CEF

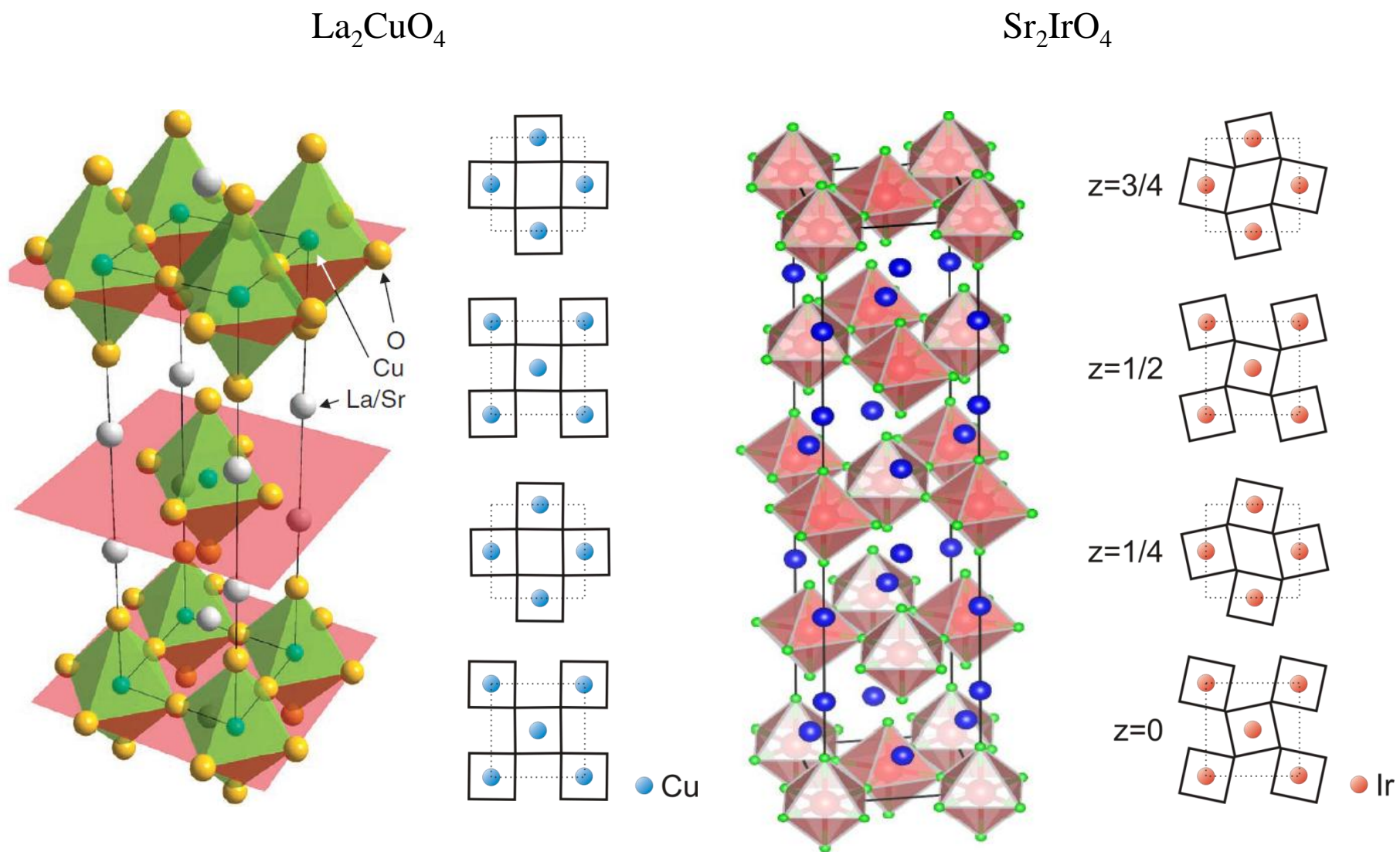


- Interplay between electron correlations, crystal electric field and spin-orbit coupling and ($U \sim \text{SOC} \sim \text{CEF}$)
- Potential for exotic physics driven by strong SOC ($\sim 0.5\text{eV}$)

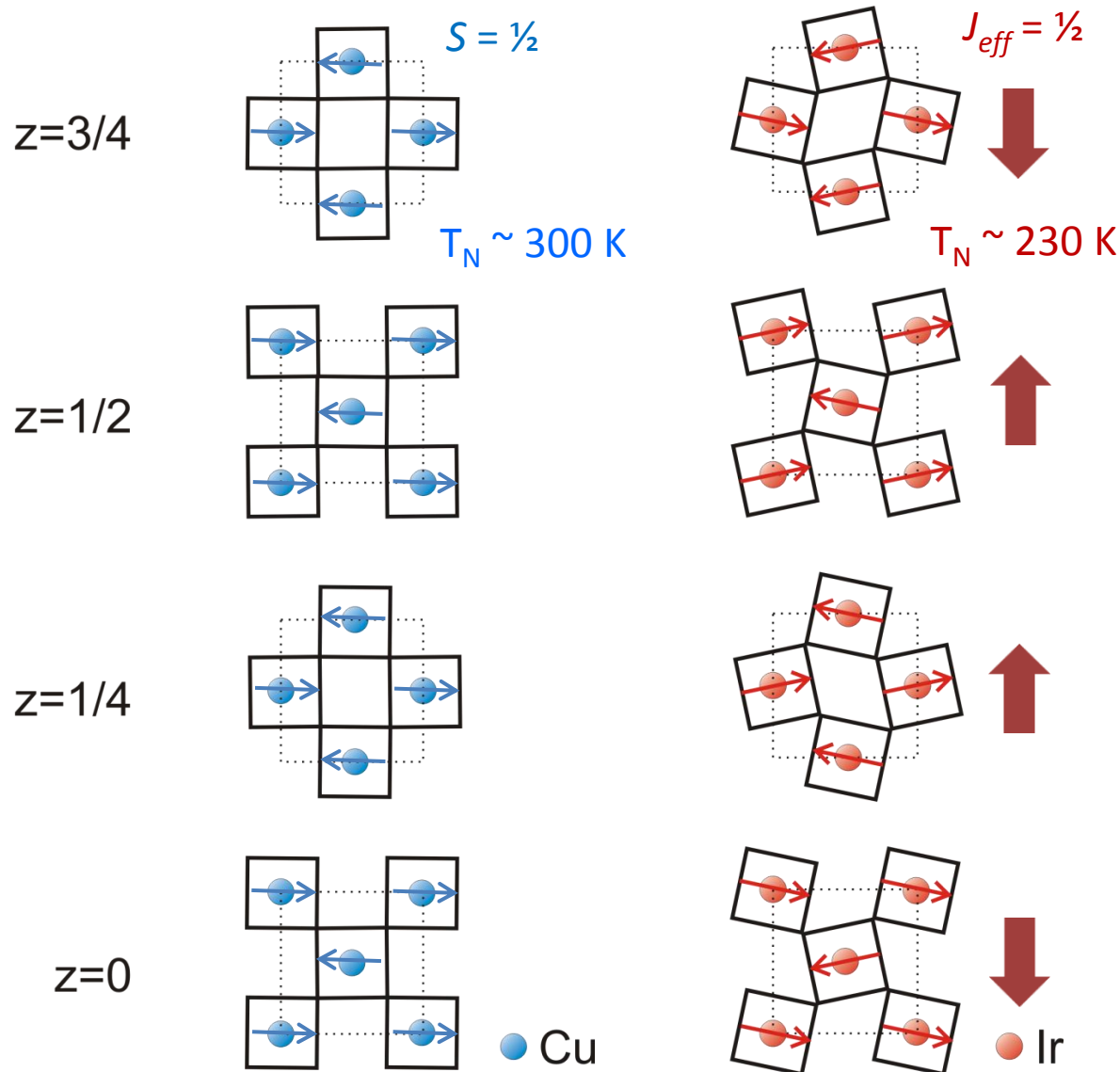
$J_{\text{eff}} = 1/2$ Mott insulators in $5d$ systems



Sr_2IrO_4 (Single-layer perovskite structure)



Sr₂IrO₄ (Orthorhombic magnetic structure)



In-plane canted dipolar AFM
 Centrosymmetric $mmm1'$

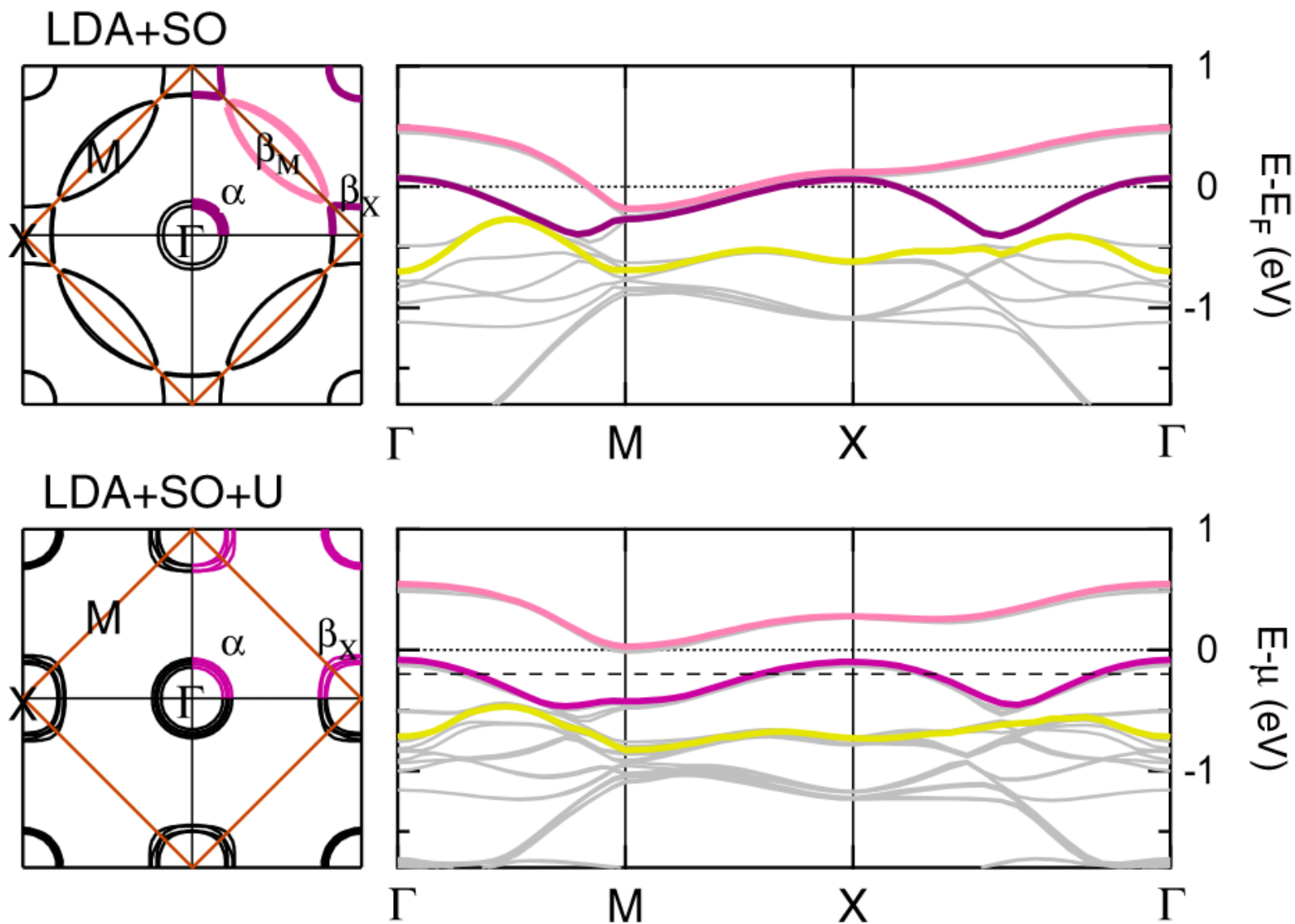
Neutron diffraction

Q. Huang *et al.*, J. Sol. State. Chem. 112, 355 (1994)
 C. Dhital *et al.*, PRB 87, 144405 (2013)
 F. Ye *et al.*, PRB 87, 140406(R) (2013)

Resonant x-ray diffraction

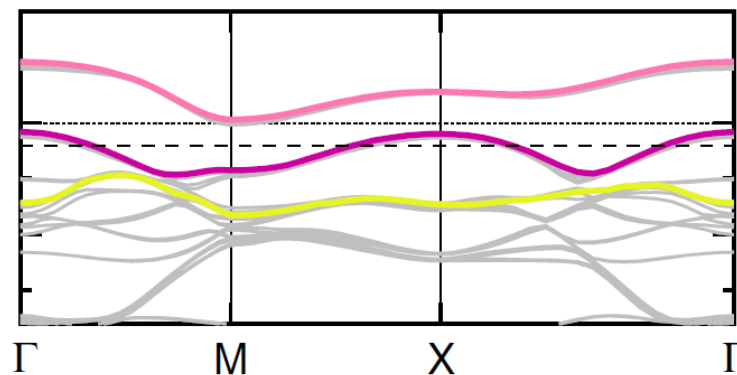
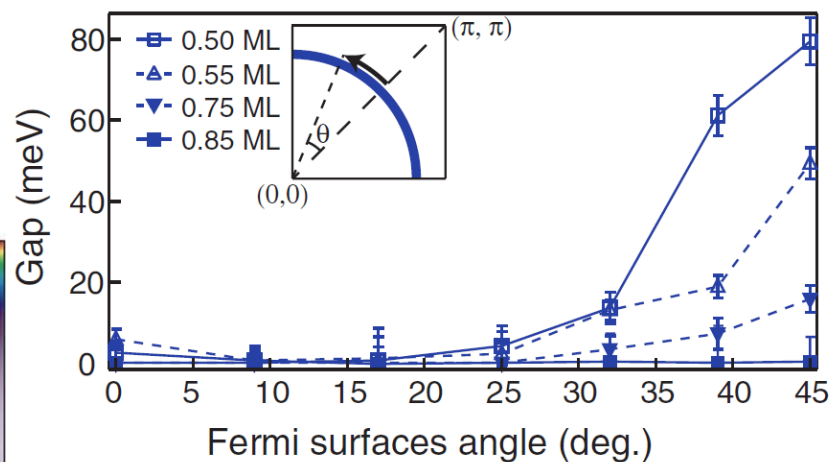
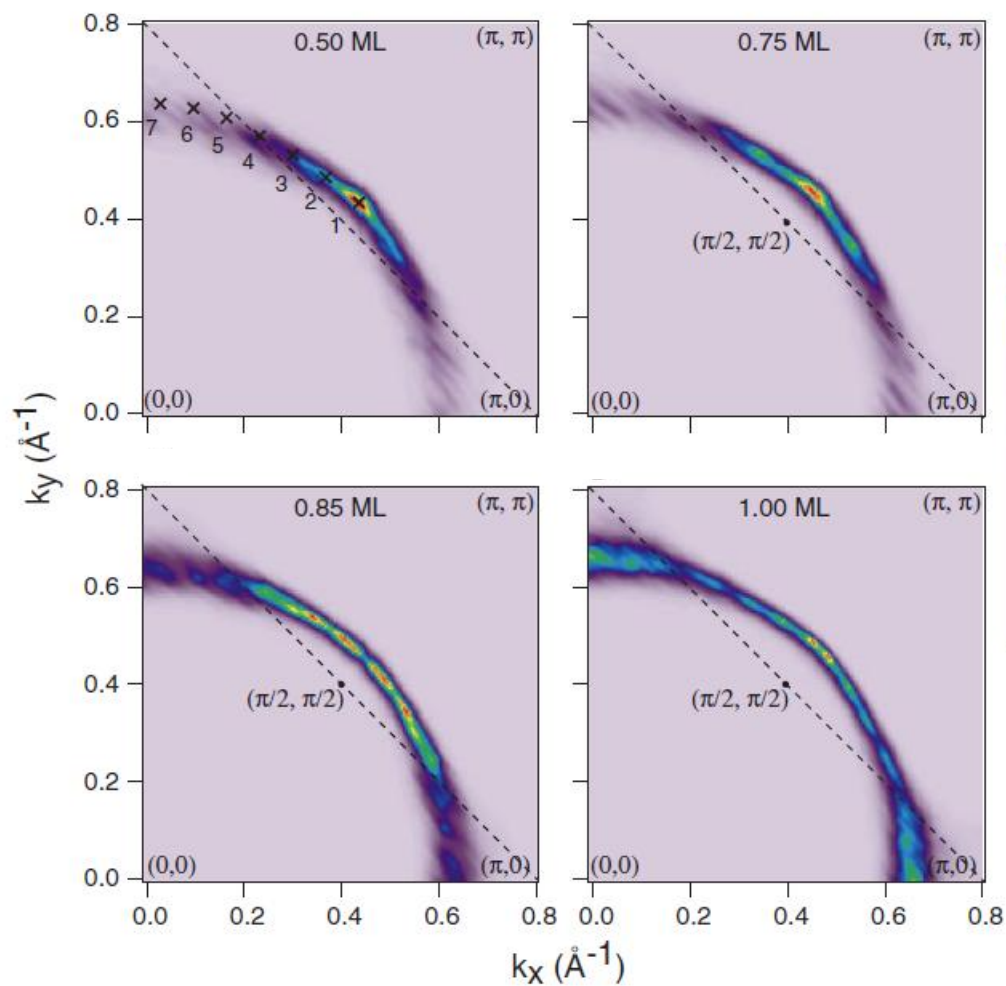
B. J. Kim *et al.*, Science, 323, 1329 (2009)
 S. Boseggia *et al.*, J. Phys. CM 25, 422202 (2013)
 S. Boseggia *et al.*, PRL 110, 117207 (2013)
 M. Moretti Sala *et al.*, PRL 112, 026403 (2014)

Sr₂IrO₄ (Electronic structure)



Fermi arcs in surface K doped Sr_2IrO_4 (electron doping)

Y. K. Kim *et al.*, Science 345, 187 (2014)

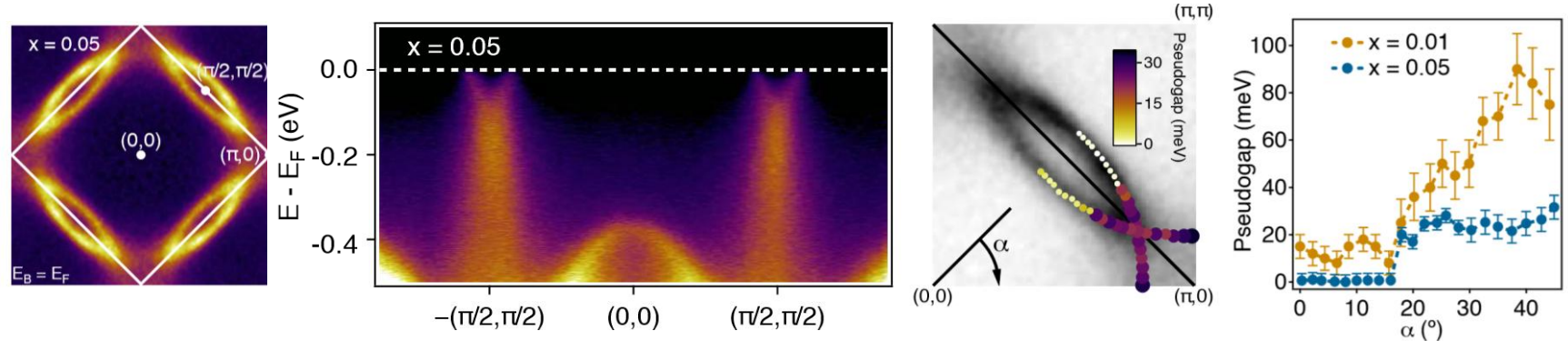


Fermi arcs and pseudogap in bulk doped Sr_2IrO_4

Observation of Fermi Arcs in ARPES measurements

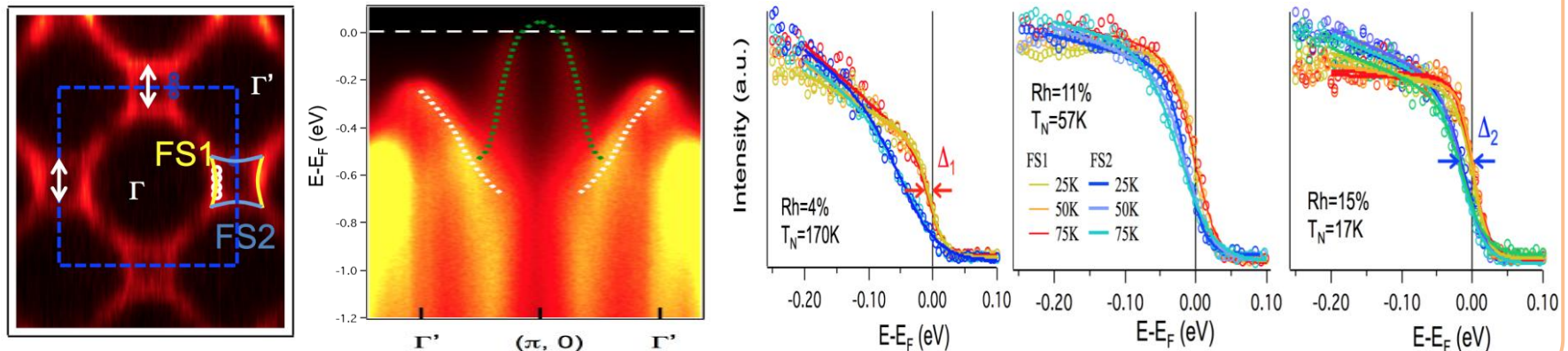
$(\text{Sr}_{1-x}\text{La}_x)_2\text{IrO}_4$ (electron doping)

A. De la Torre *et al.*, <http://arxiv.org/abs/1506.00616> (2015)

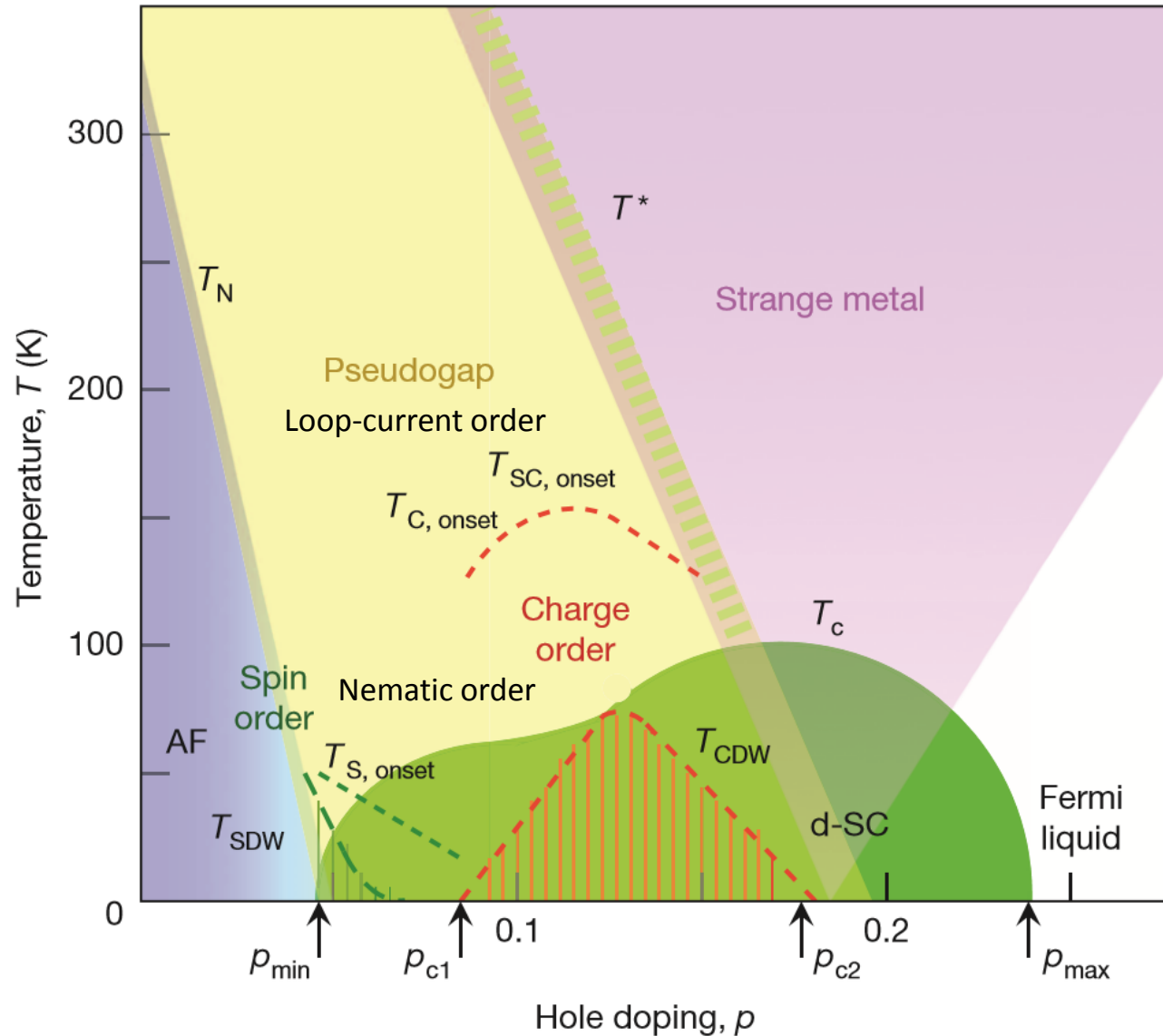


$\text{Sr}_2\text{Ir}_{1-x}\text{Rh}_x\text{O}_4$ (hole doping)

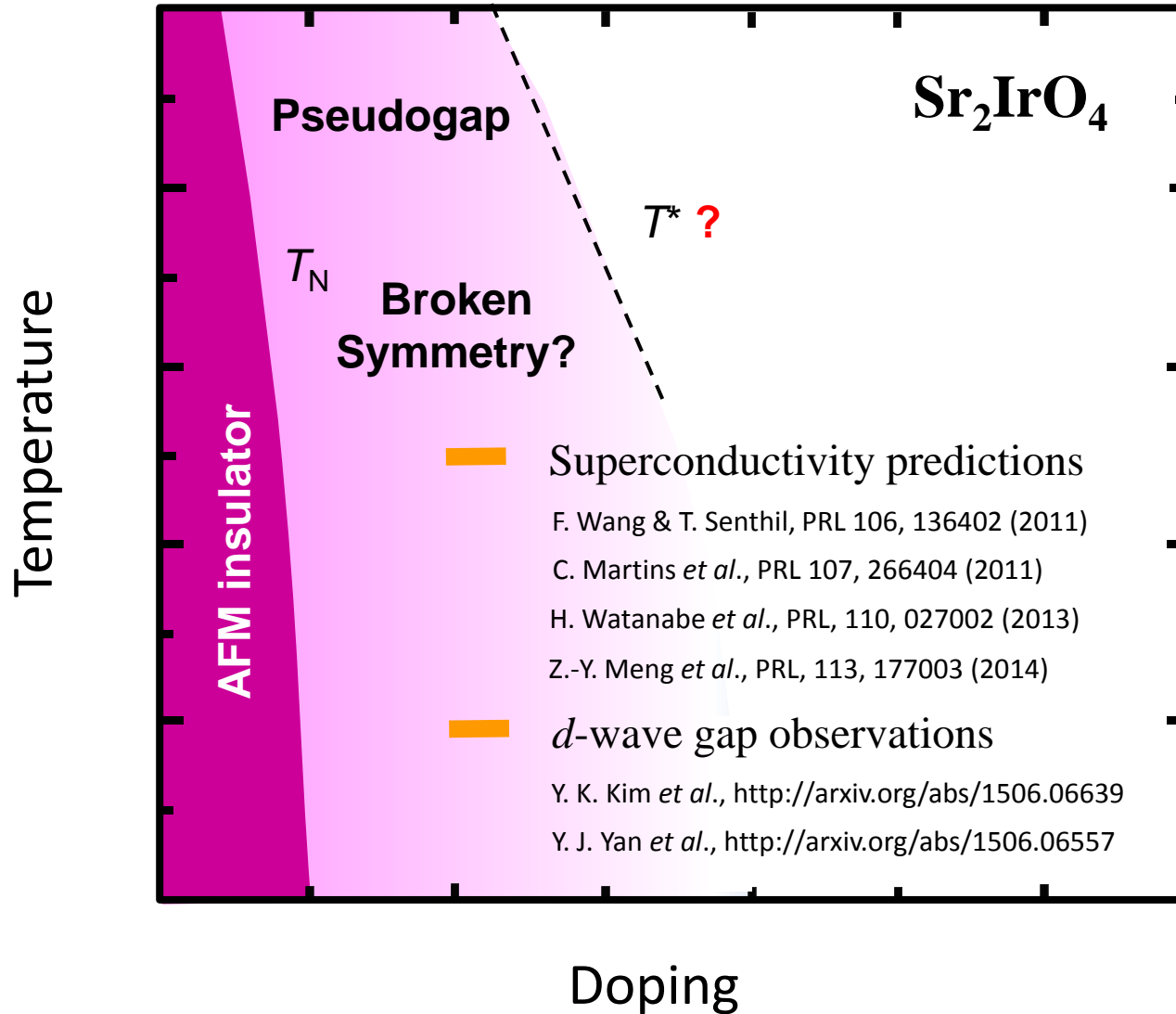
Y. Cao *et al.*, <http://arxiv.org/abs/1406.4978> (2014)



Broken symmetry phases proximate to AF order in cuprates

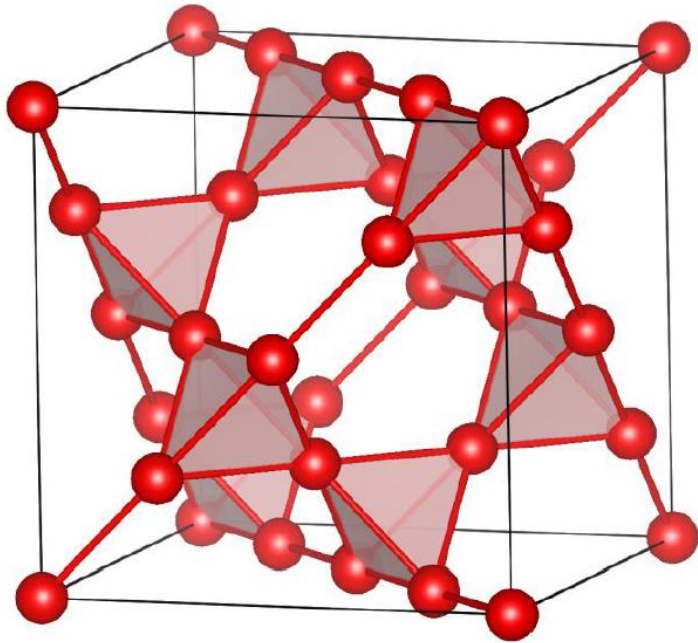


Exotic phases in iridates?



Neumann's principle

A tensor describing any physical property of a crystal must be invariant under all symmetry operations of the crystal



- If $\chi_{ijk\dots n}$ is a property tensor
- and T_{ip} is an element in the symmetry group of the crystal
- then:
$$\chi_{ijk\dots n} = T_{ip}T_{jq}T_{kr} \dots T_{nu}\chi_{pqr\dots u}$$
- The set of relationships between χ 's greatly reduced the number of non-zero independent tensor components

Higher rank tensors → greater symmetry resolution

$$\chi_{ij}^{(1)}$$

$$\chi_{ijk}^{(2)}$$

$$\chi_{ijkl}^{(3)}$$

Tetragonal	# elem.
Trigonal	
Hexagonal	

$$\begin{bmatrix} xx & 0 & 0 \\ 0 & xx & 0 \\ 0 & 0 & zz \end{bmatrix}$$

$$4 = C_4 \quad 7$$

$$\bar{4} = S_4 \quad 6$$

$$422 = D_4 \quad 3$$

$$4mm = C_{4v} \quad 4$$

$$\bar{4}2m = D_{2d} \quad 3^*$$

$$4/m = C_{4h} \quad 0$$

$$4/mmm = D_{4h} \quad 0$$

$$4 = C_4 \quad 21$$

$$\bar{4} = S_4 \quad 21$$

$$422 = D_4 \quad 11$$

$$4mm = C_{4v} \quad 11$$

$$\bar{4}2m = D_{2d} \quad 11$$

$$4/m = C_{4h} \quad 21$$

$$4/mmm = D_{4h} \quad 11$$

Nonlinear optics

Multiple expansion of radiation source term

$$\vec{S} \propto \mu_0 \frac{\partial^2 \vec{P}}{\partial t^2} + \mu_0 \left(\vec{\nabla} \times \frac{\partial \vec{M}}{\partial t} \right) - \mu_0 \left(\vec{\nabla} \frac{\partial^2 \hat{Q}}{\partial t^2} \right) + \dots$$

Expansion of electric dipole (P), magnetic dipole (M) and electric quadrupole (Q) contributions

$$P_i = \chi_{ij}^{ee} E_j(\omega) + \chi_{ij}^{em} H_j(\omega) + \chi_{ijk}^{eee} E_j(\omega) E_k(\omega) + \chi_{ijk}^{eem} E_j(\omega) H_k(\omega) + \chi_{ijk}^{emm} H_j(\omega) H_k(\omega) + \dots$$

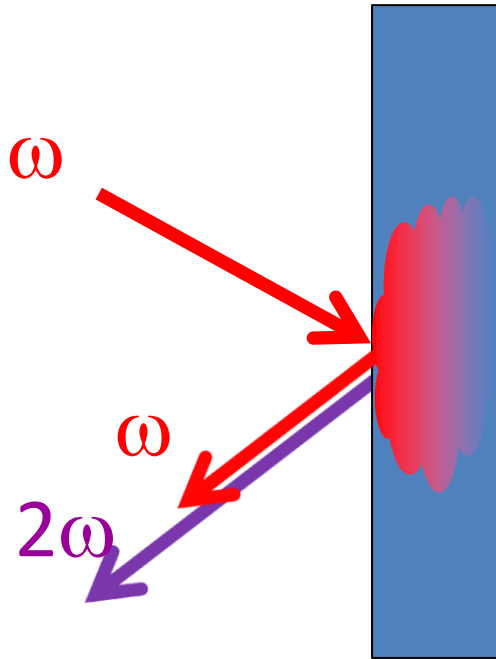
$$M_i = \chi_{ij}^{me} E_j(\omega) + \chi_{ij}^{mm} H_j(\omega) + \chi_{ijk}^{mee} E_j(\omega) E_k(\omega) + \chi_{ijk}^{mem} E_j(\omega) H_k(\omega) + \chi_{ijk}^{mmm} H_j(\omega) H_k(\omega) + \dots$$

$$\hat{Q}_{ij} = \chi_{ijk}^{qe} E_k(\omega) + \chi_{ijk}^{qm} H_k(\omega) + \chi_{ijkl}^{qee} E_k(\omega) E_l(\omega) + \chi_{ijkl}^{qem} E_k(\omega) H_l(\omega) + \chi_{ijkl}^{qmm} H_k(\omega) H_l(\omega) + \dots$$

1st order responses

2nd order responses

Optical second harmonic generation (SHG)



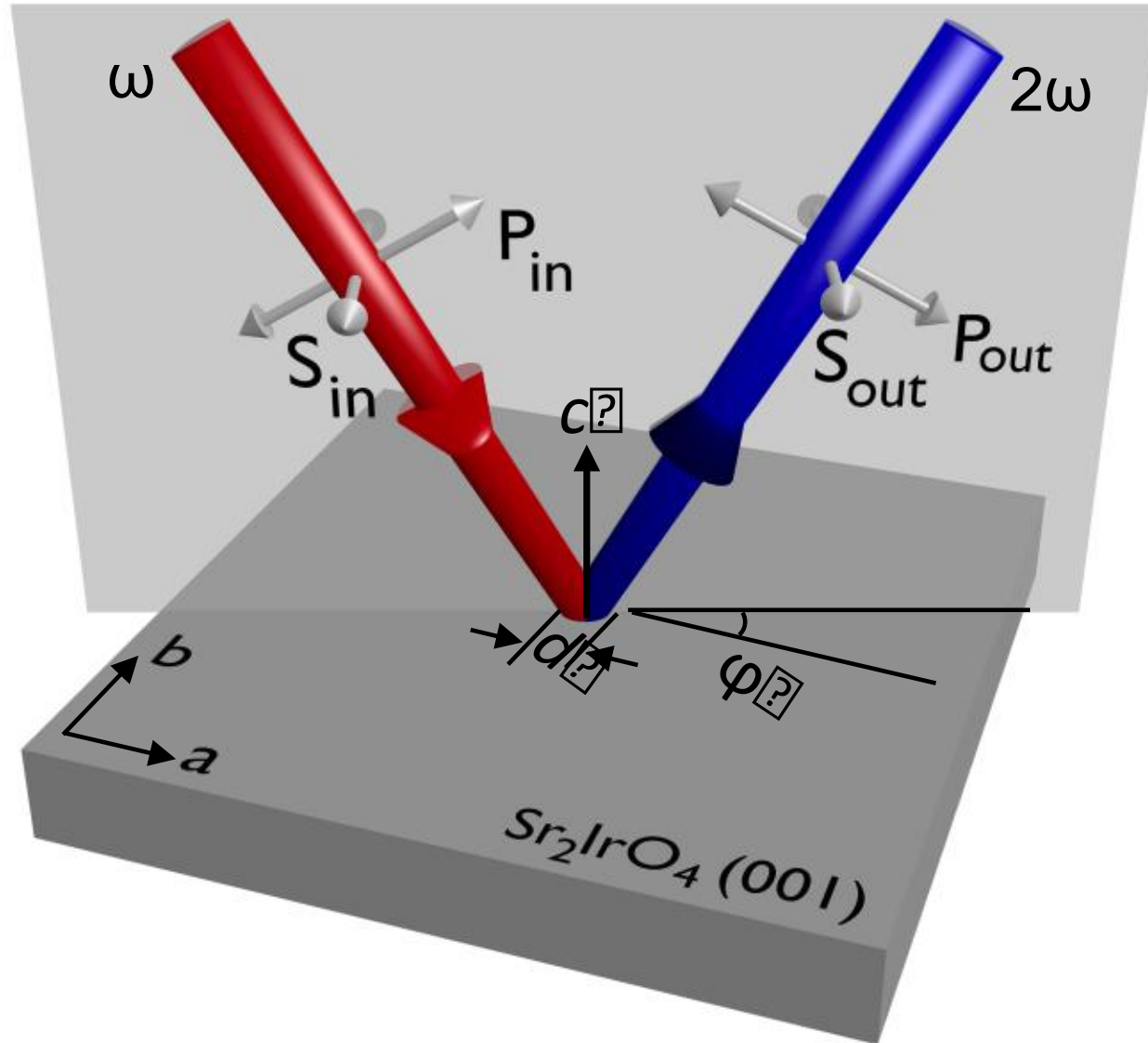
$$P_i(\omega) = \chi_{ij}^{ED} E_j(\omega)$$

$$P_i(2\omega) = \chi_{ijk}^{ED} E_j(\omega) E_k(\omega) \\ + \chi_{ijkl}^{EQ} E_j(\omega) \nabla_k E_l(\omega) \\ + \dots$$

$\chi_{ijk}^{ED} = 0$ if system has inversion symmetry

$\chi_{ijkl}^{EQ} \neq 0$ even if system has inversion symmetry
much weaker than ED contribution ($\sim \lambda/a$)

Rotational anisotropy



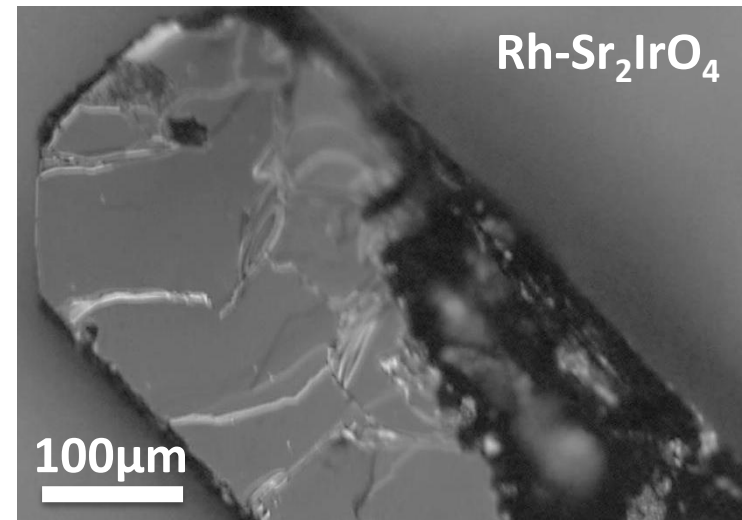
Technical limitations of conventional rotational anisotropy

Alignment problems:

- Beam walk on sample
- Precession of reflected light
- Need large area flat single crystals (e.g. thin-film, polishing)

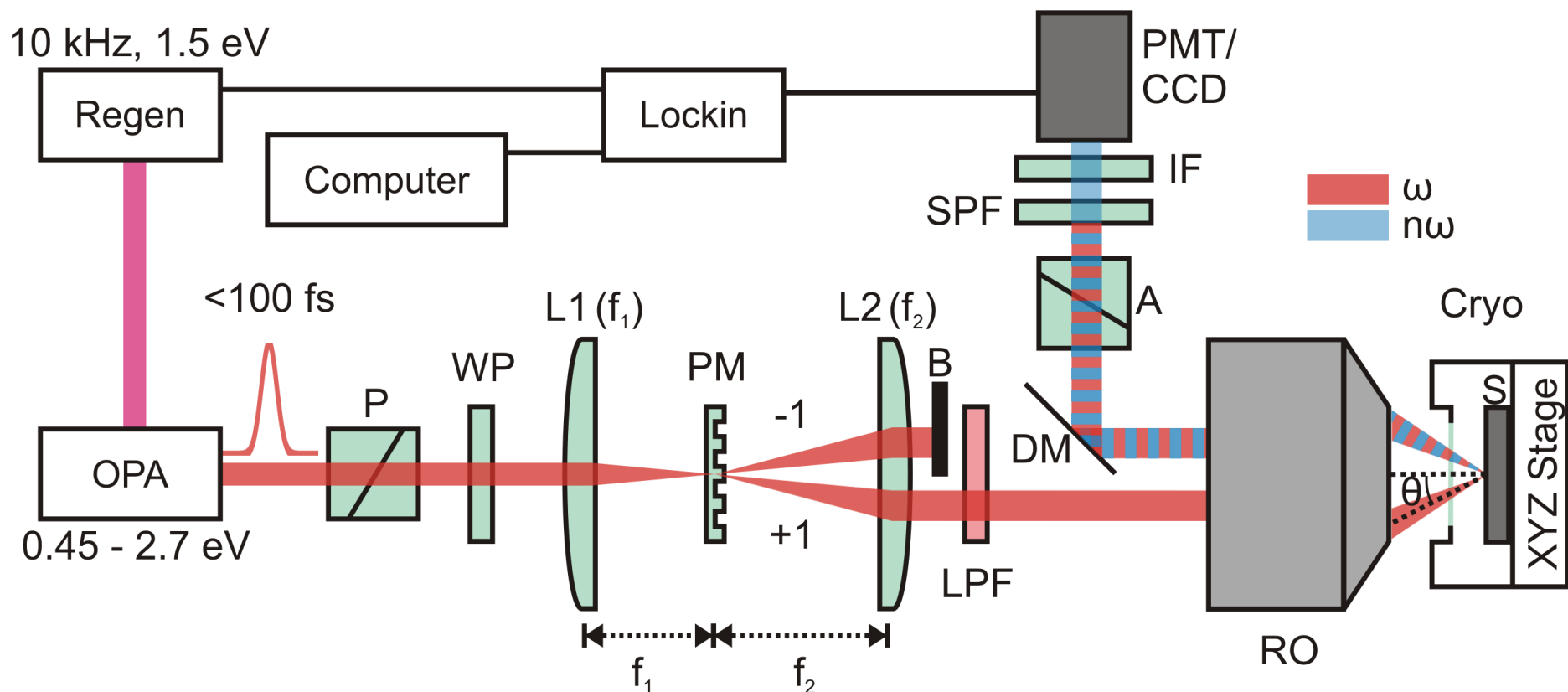
Need for rotating sample creates additional challenges for:

- Cryogenic measurements
- Magnetic field measurements
- Strained samples
- Imaging measurements



Rotating scattering plane based RA-SHG

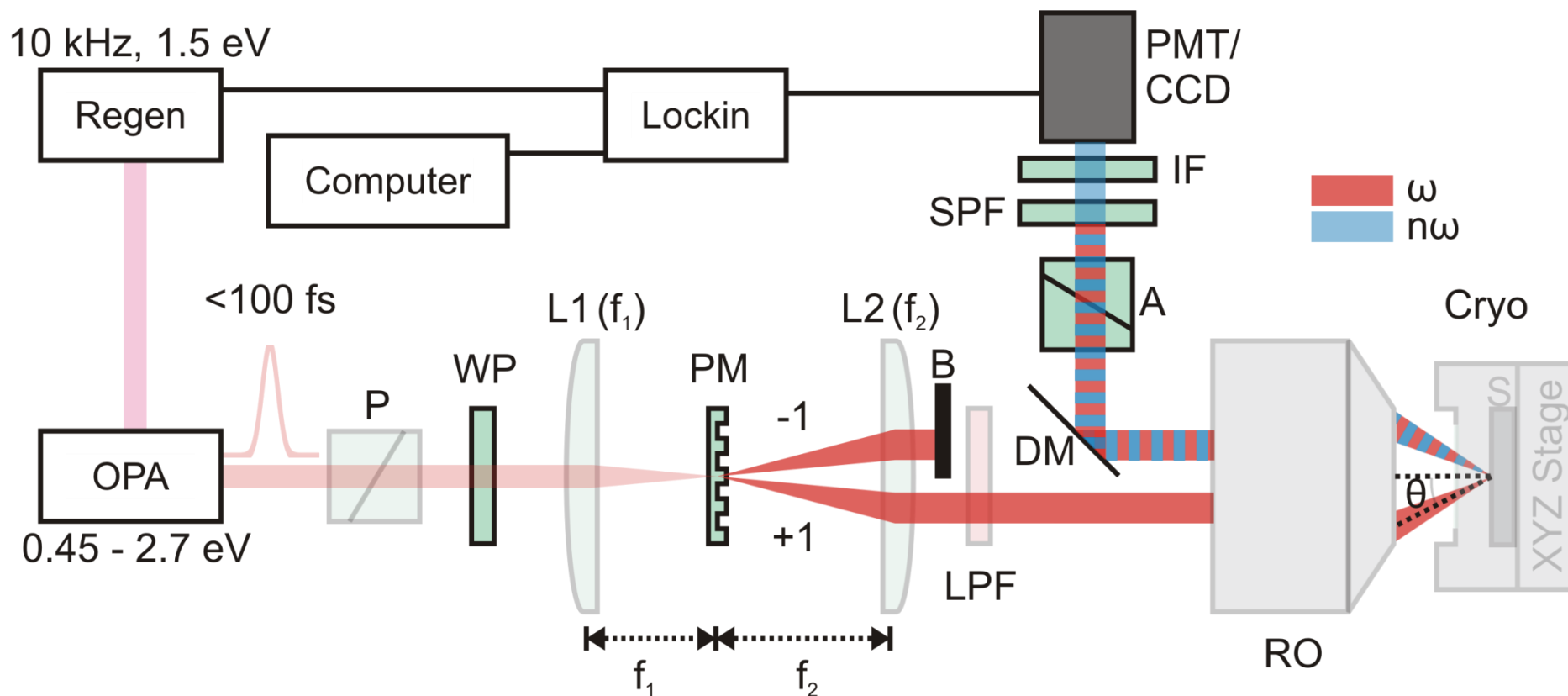
Instead of rotating the sample, the scattering plane is rotated.



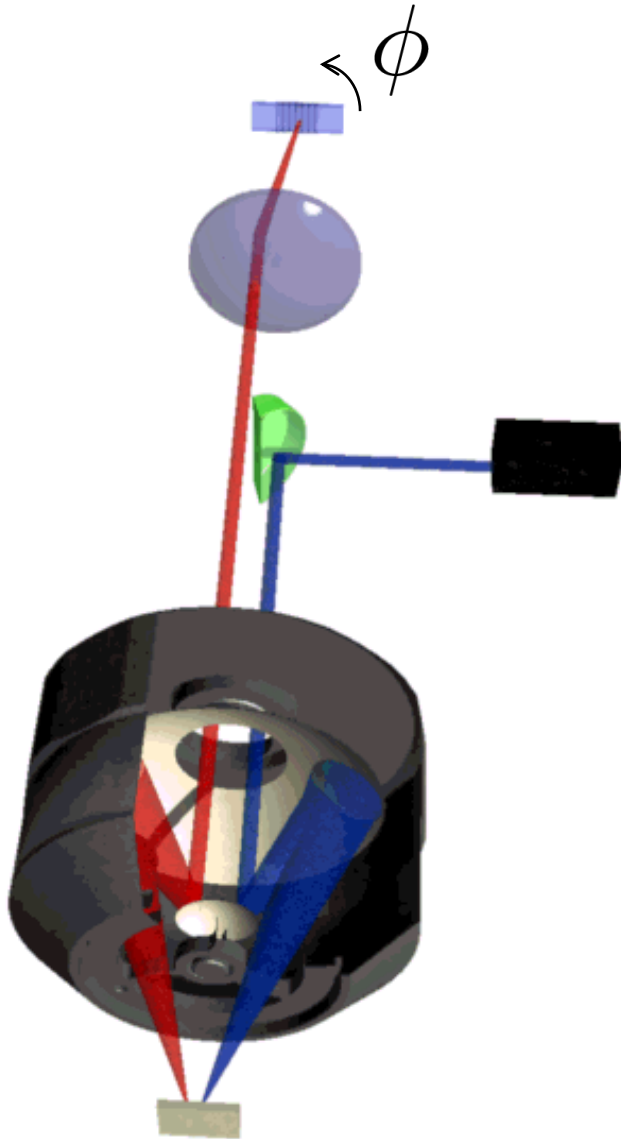
Measurement is performed at oblique angle θ ✓

Rotating scattering plane based RA-SHG

Only a handful of optics rotate.



Rotating scattering plane based RA-SHG

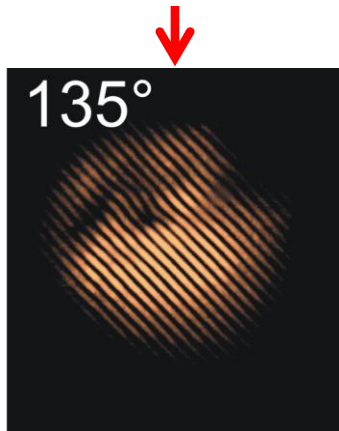
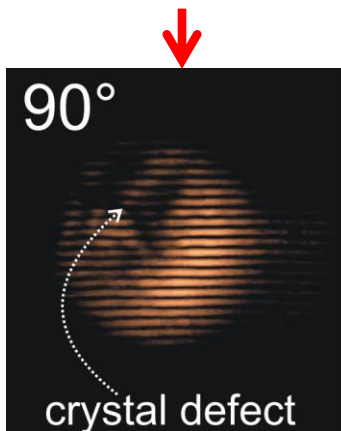
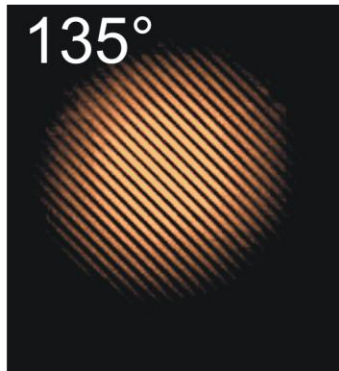
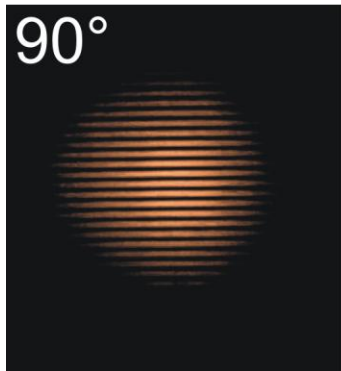
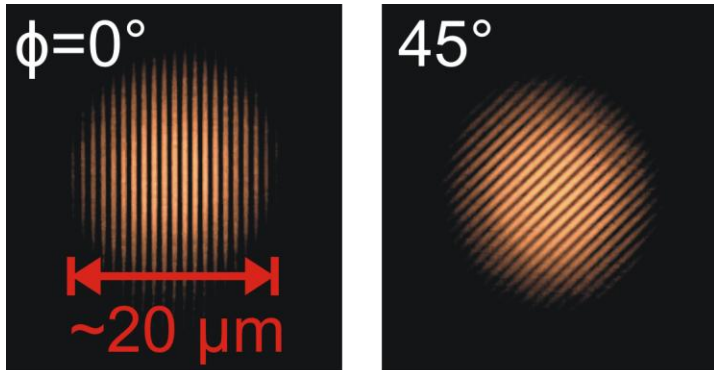


Sample is totally stationary.

Thus, we may perform measurements:

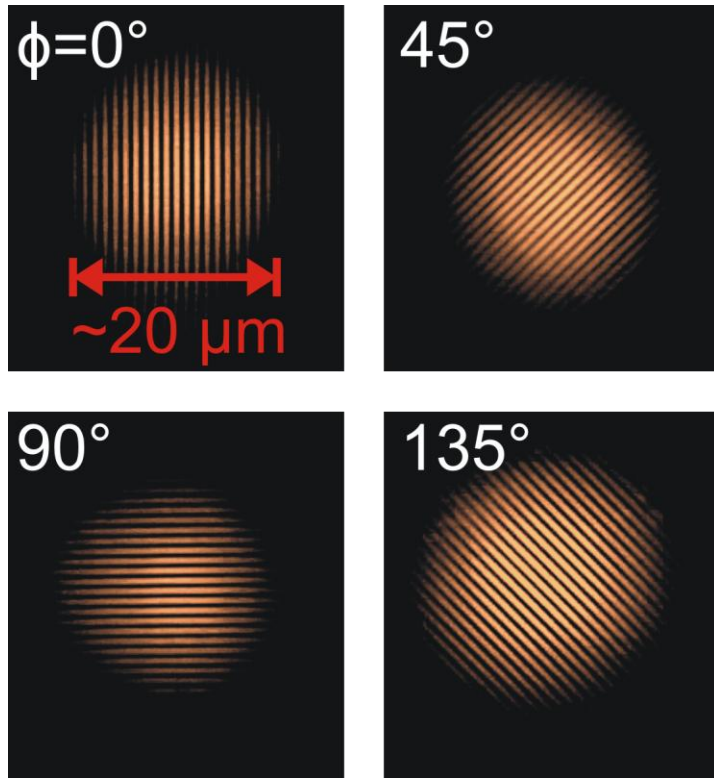
- in ultracold environments ✓
- in a magnetic field ✓
- on small single crystals ✓
- as a scanning experiment ✓

Characterization of spot size and local repeatability

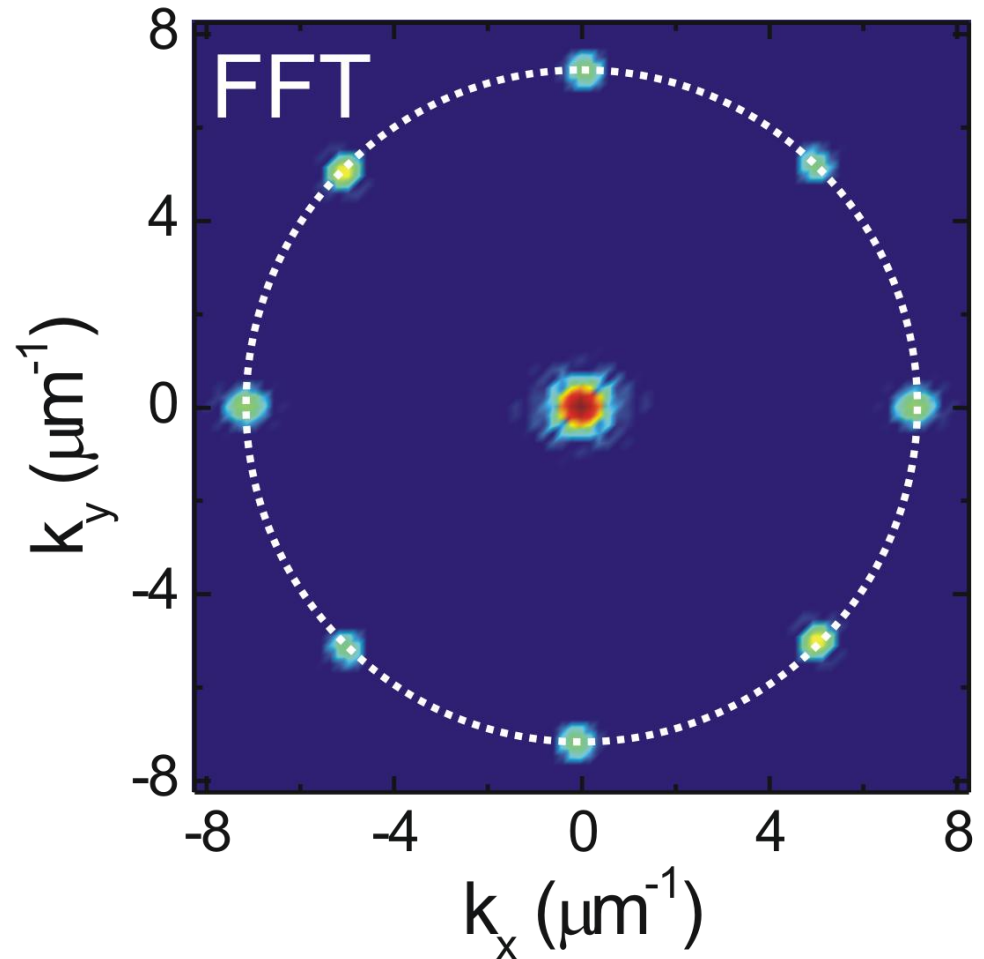


- Beam walking on sample $\sim 1 \mu\text{m}$
- Always measure the same portion of the sample ✓

Characterization of scattering angle precession



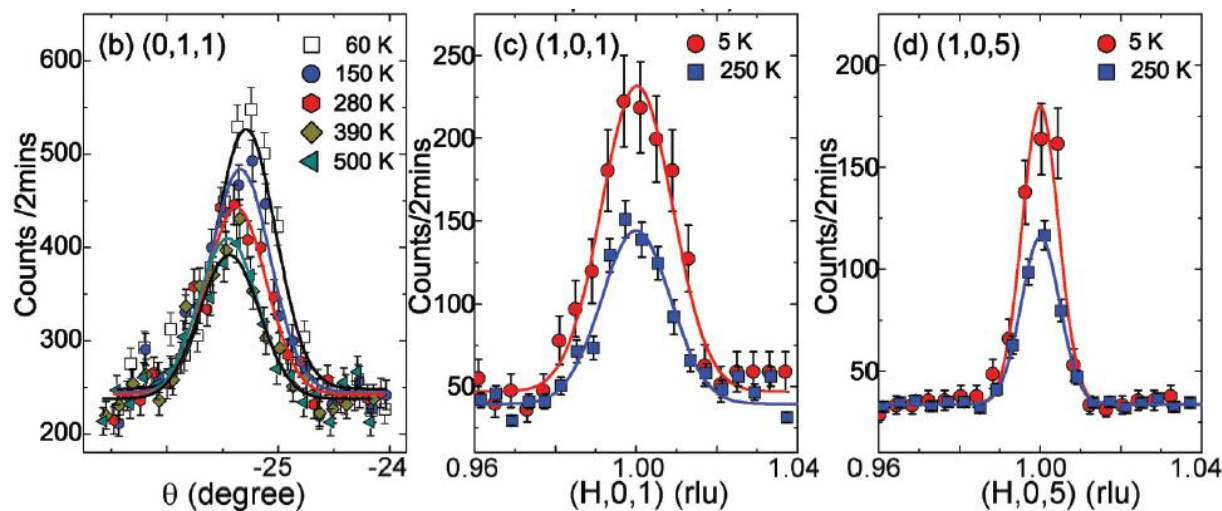
$$\Lambda = \frac{\lambda}{2 \sin(\theta)} \sim 900 \text{ nm}$$



Precession of scattering plane with respect to surface normal $< 0.05^\circ$ ✓

Structural symmetry

Unexplained forbidden neutron peaks



(1994 – 2013) space group $I4_1/acd$

M. K. Crawford *et al.*, PRB 49, 9198 (1994)

Q. Huang *et al.*, J. Sol. State. Chem. 112, 355 (1994)

B. J. Kim *et al.*, Science, 323, 1329 (2009)

(2013) $(h = 2n, 0, l = 2n)$ peaks observed

Violation of $I4_1/acd$

Structural defects?

Spatial inhomogeneity?

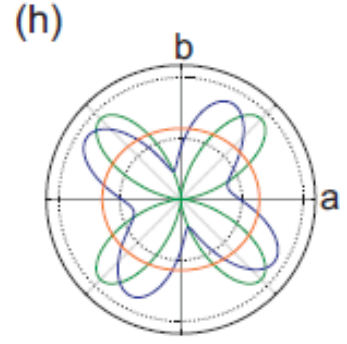
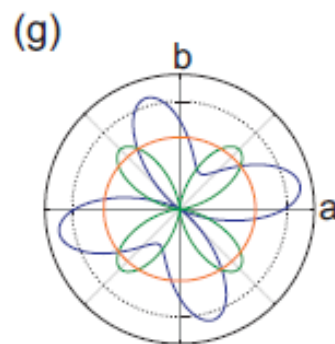
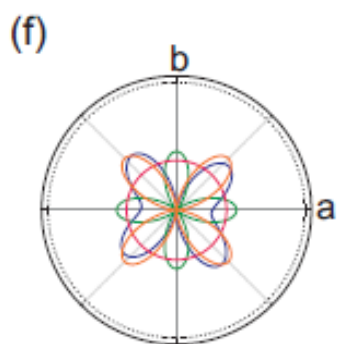
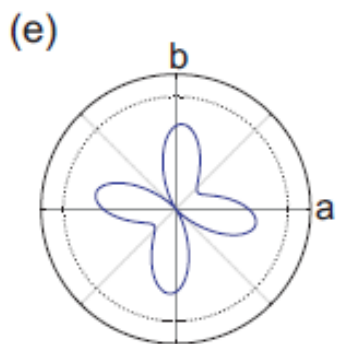
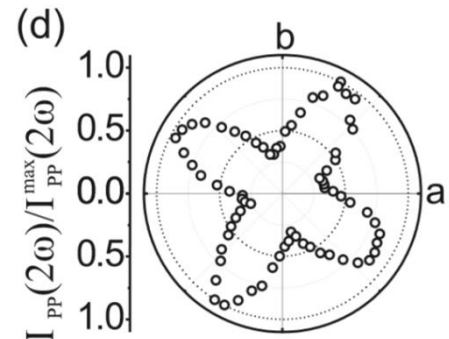
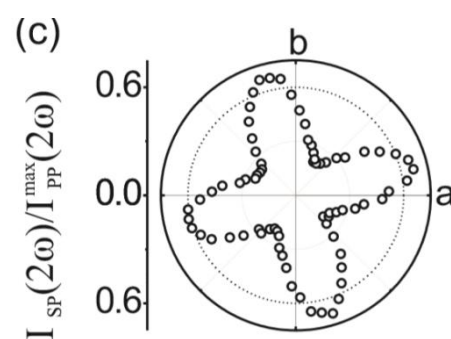
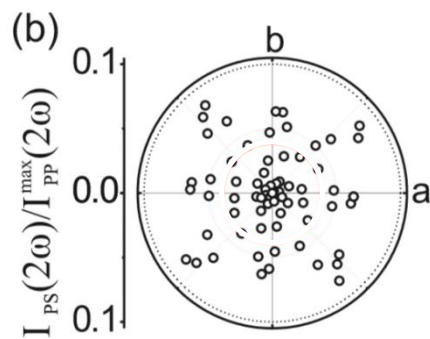
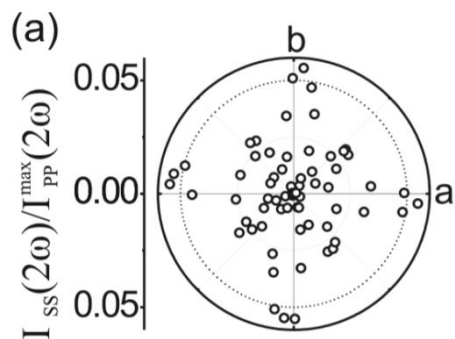
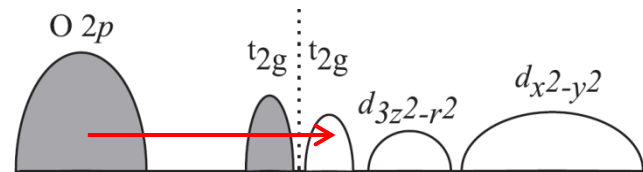
Lower crystal symmetry?

C. Dhital *et al.*, PRB 87, 144405 (2013)

F. Ye *et al.*, PRB 87, 140406(R) (2013)

Second harmonic generation from Sr₂IrO₄ (001)

$\lambda_{in} = 800$ nm
 $\lambda_{out} = 400$ nm



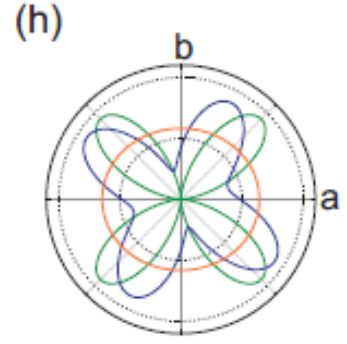
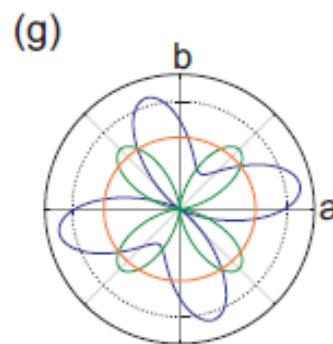
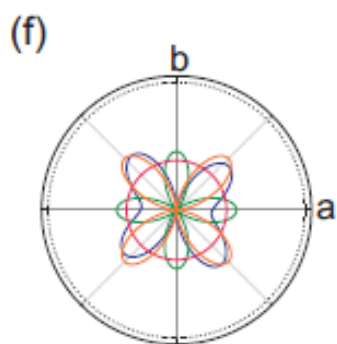
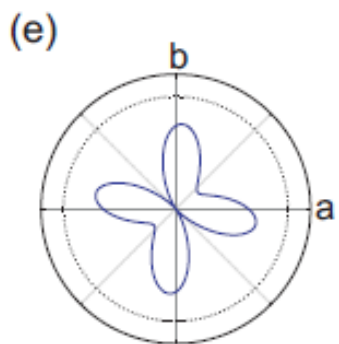
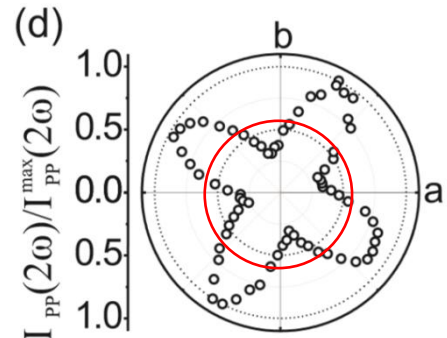
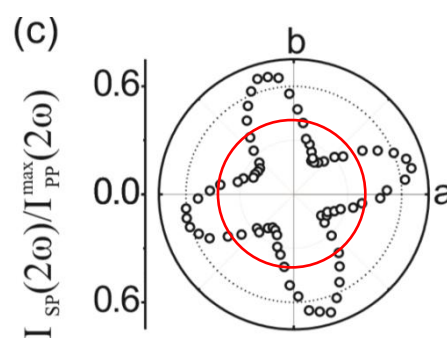
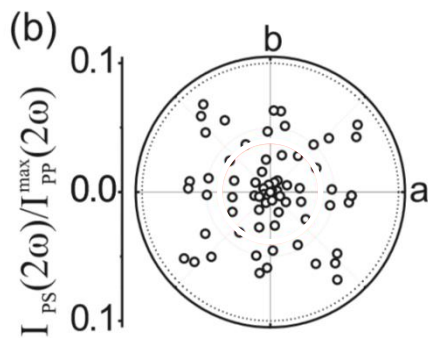
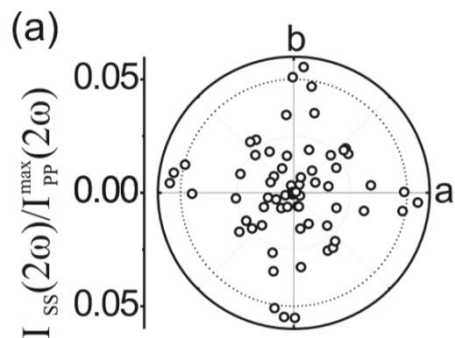
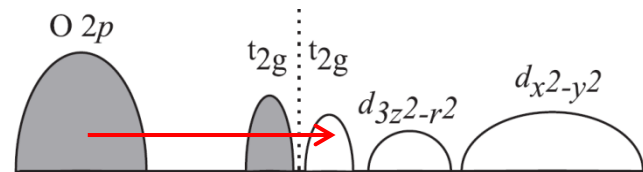
Non-centrosymmetric (bulk ED)

— C_s — D₂ — D₄

Proposed

Second harmonic generation from Sr₂IrO₄ (001)

$\lambda_{in} = 800 \text{ nm}$
 $\lambda_{out} = 400 \text{ nm}$



Centrosymmetric (surface ED)

Non-centrosymmetric (bulk ED)

Proposed



D_{4h}



C_s



D₂

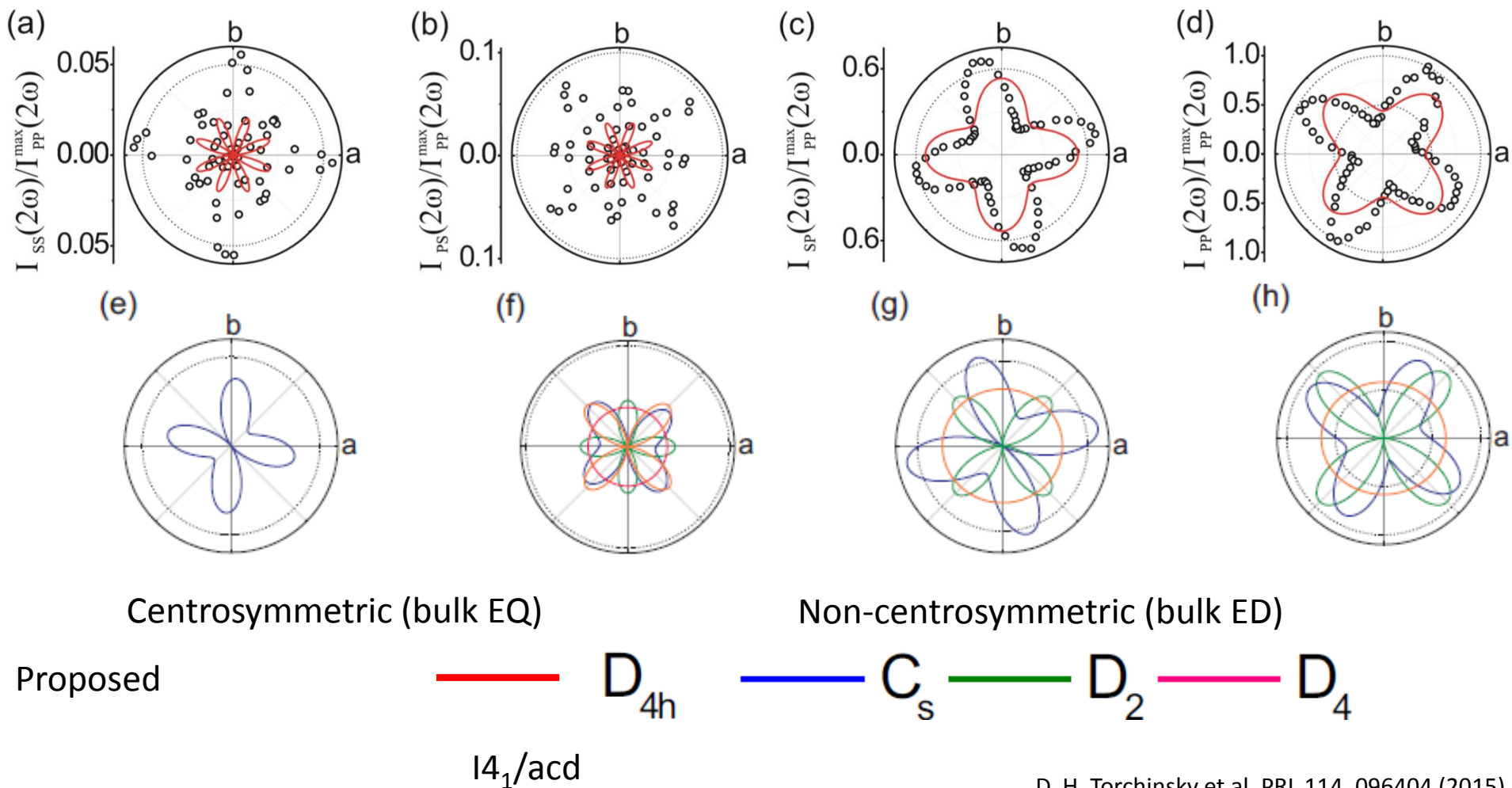
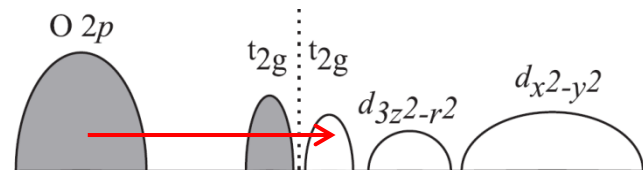


D₄

I4₁/acd

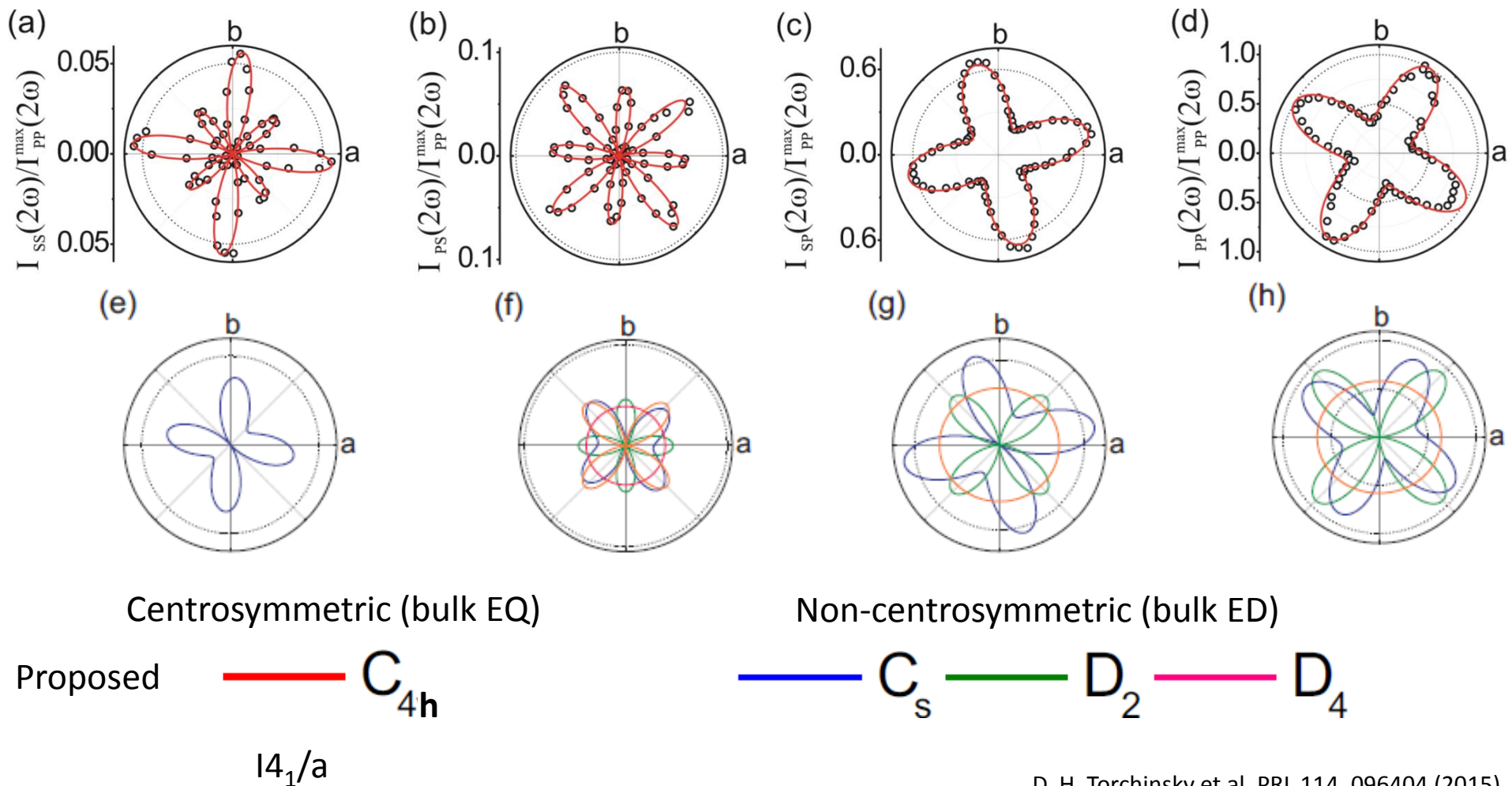
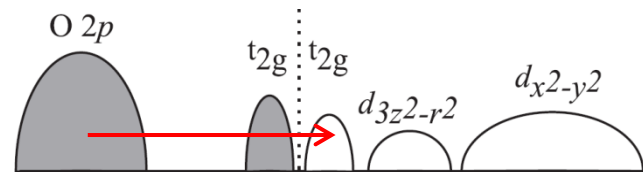
Second harmonic generation from Sr₂IrO₄ (001)

$\lambda_{in} = 800 \text{ nm}$
 $\lambda_{out} = 400 \text{ nm}$

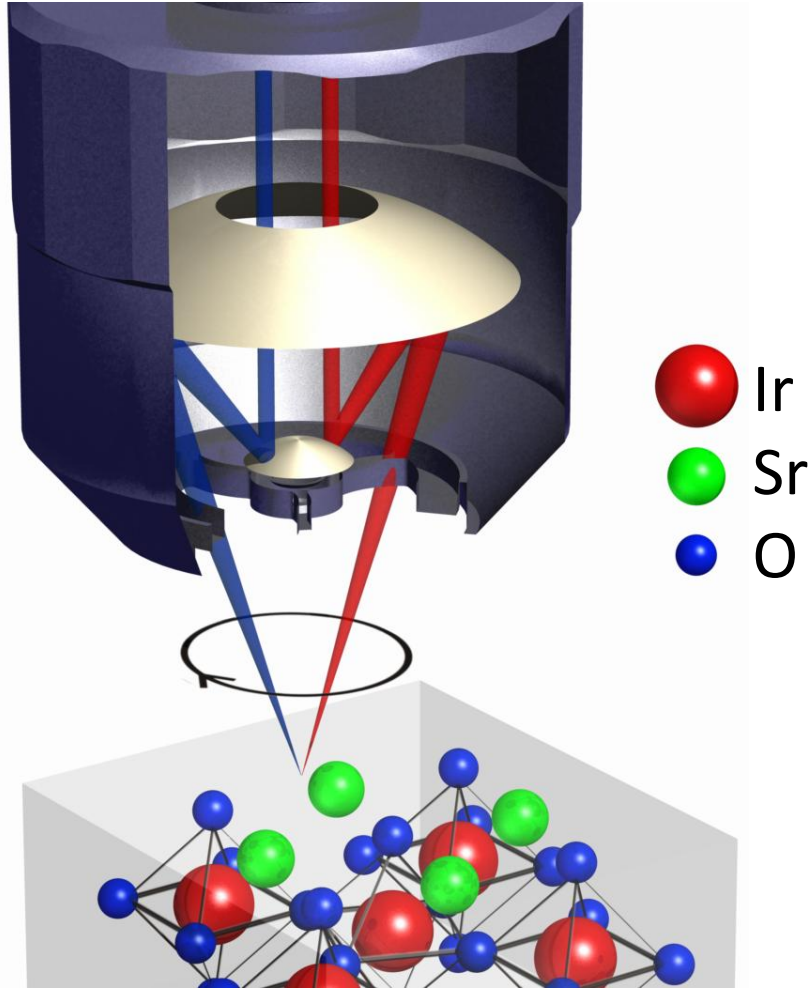


Second harmonic generation from Sr₂IrO₄ (001)

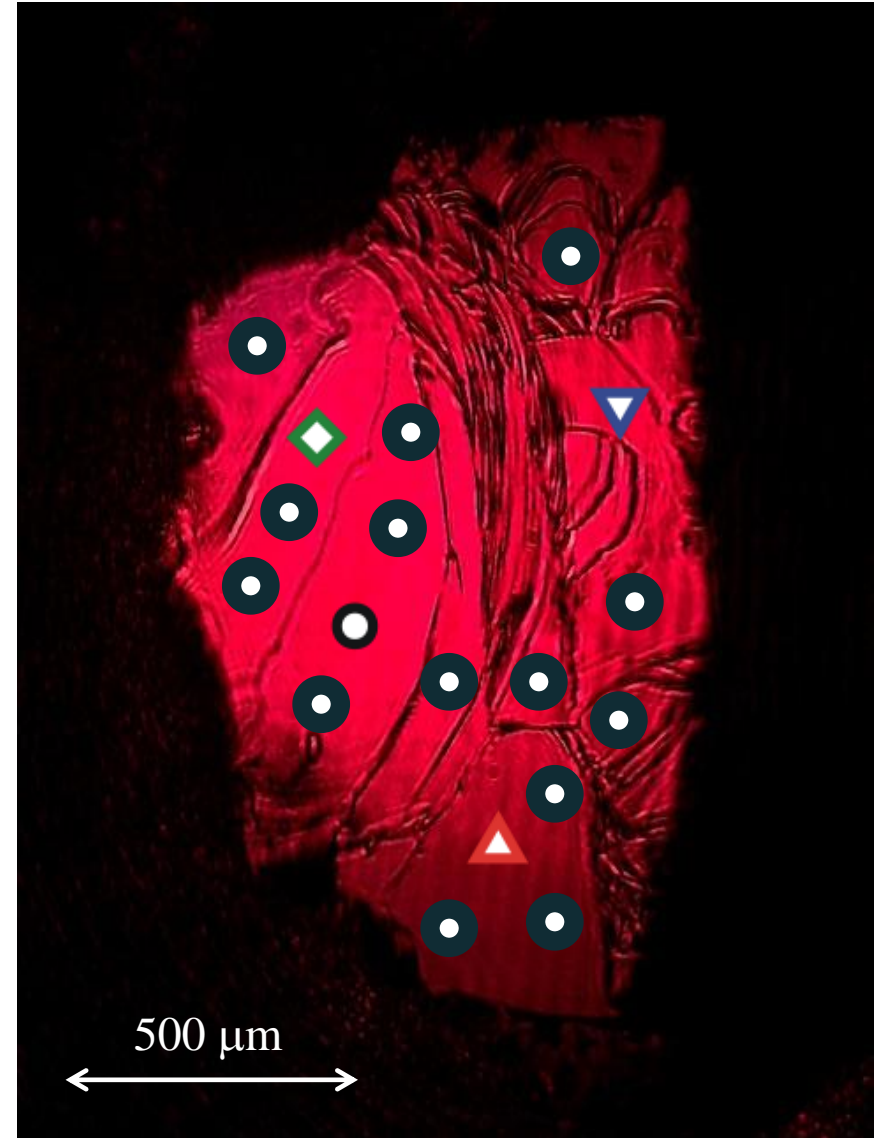
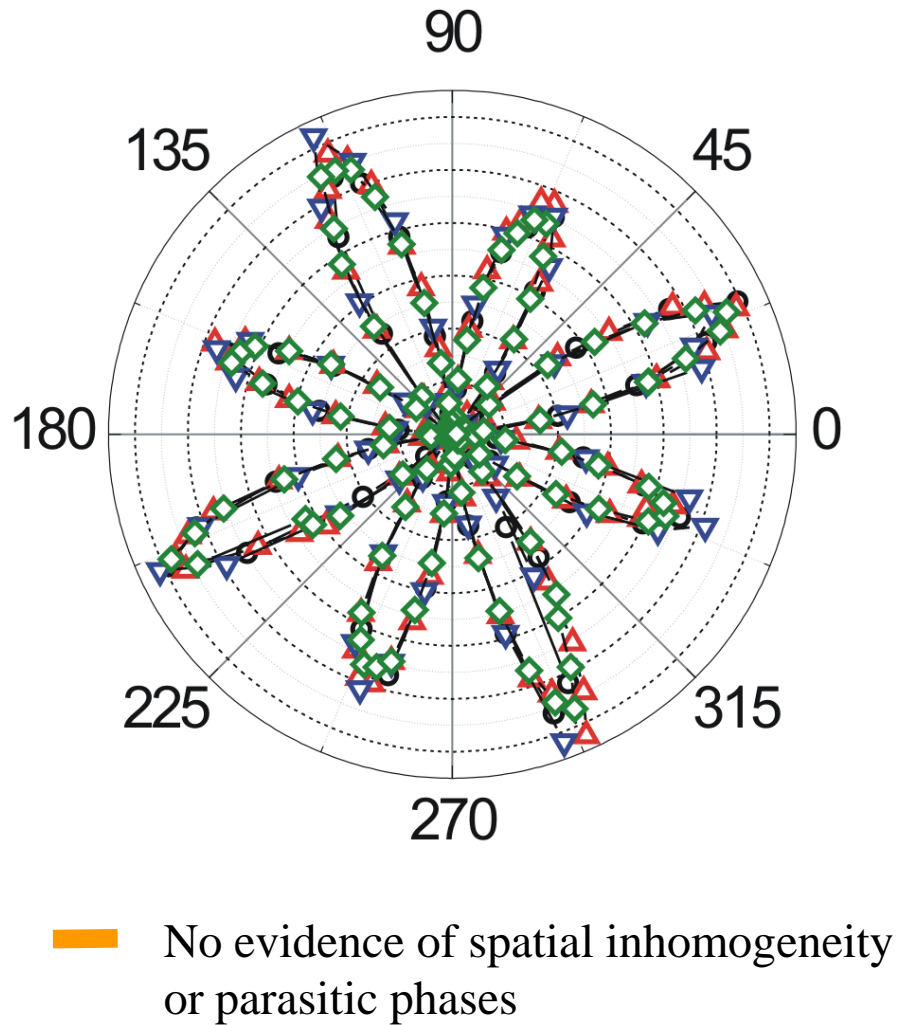
$\lambda_{in} = 800 \text{ nm}$
 $\lambda_{out} = 400 \text{ nm}$



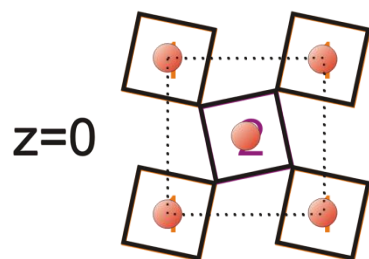
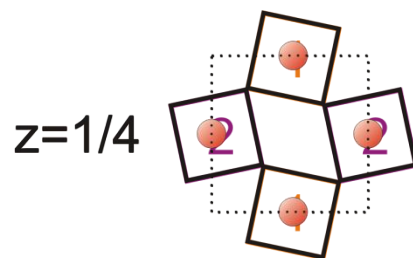
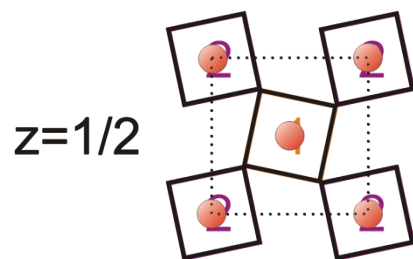
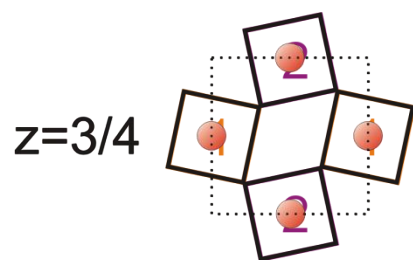
Nonlinear optical microscopy



Spatially resolved symmetry mapping

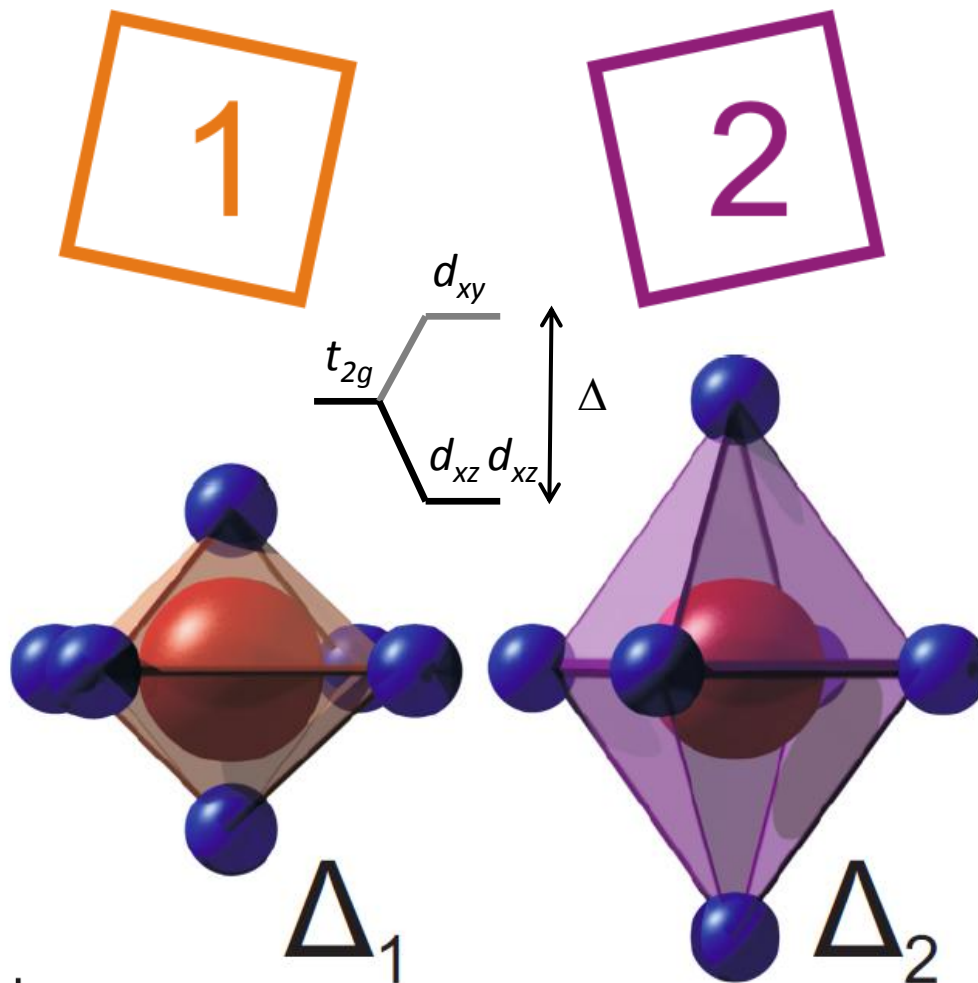


Lowered global symmetry $I4_1/acd \rightarrow I4_1/a$



● Ir

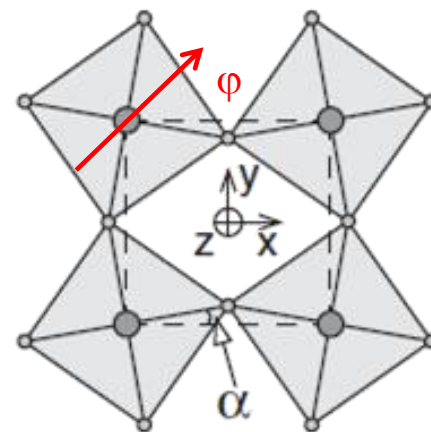
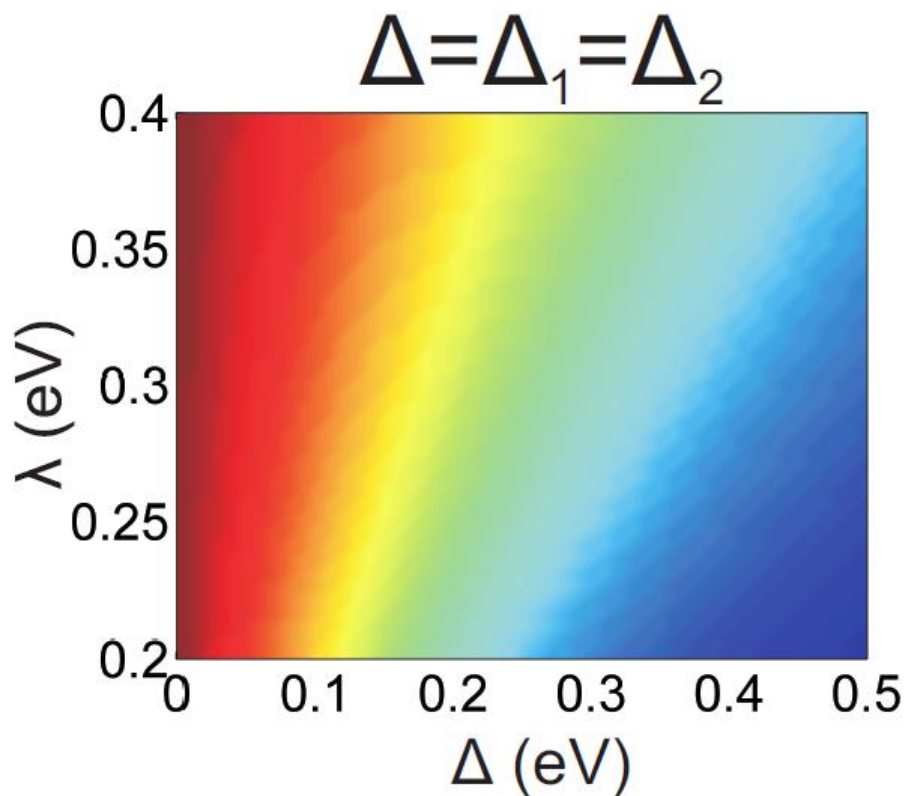
Loss of c, d glide planes from $I4_1/acd \rightarrow I4_1/a$ occurs via staggered tetragonal distortion



Consequences of lowered global symmetry

D. H. Torchinsky et al. PRL 114, 096404 (2015)

$$H = \sum_{n,n'} J \mathbf{S}_n \mathbf{S}_{n'} - D(S_n^x S_{n'}^y - S_n^y S_{n'}^x) \\ + \delta J_z S_n^z S_{n'}^z + \delta J_{xy} (\mathbf{S}_n \cdot \mathbf{r}_{n,n'}) (\mathbf{S}_{n'} \cdot \mathbf{r}_{n,n'})$$



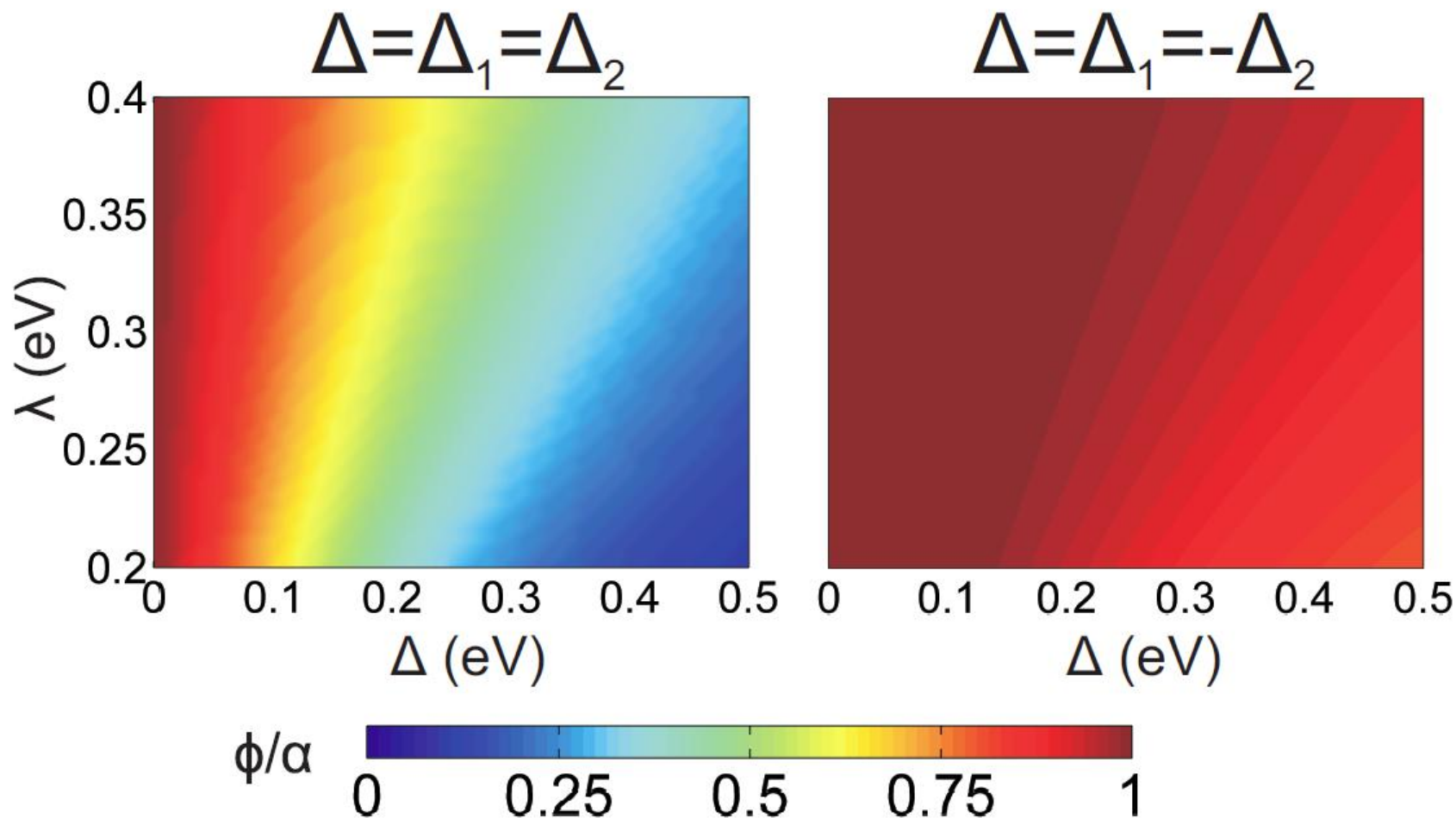
G. Jackeli and G. Khaliullin PRL 102, 017205 (2009)

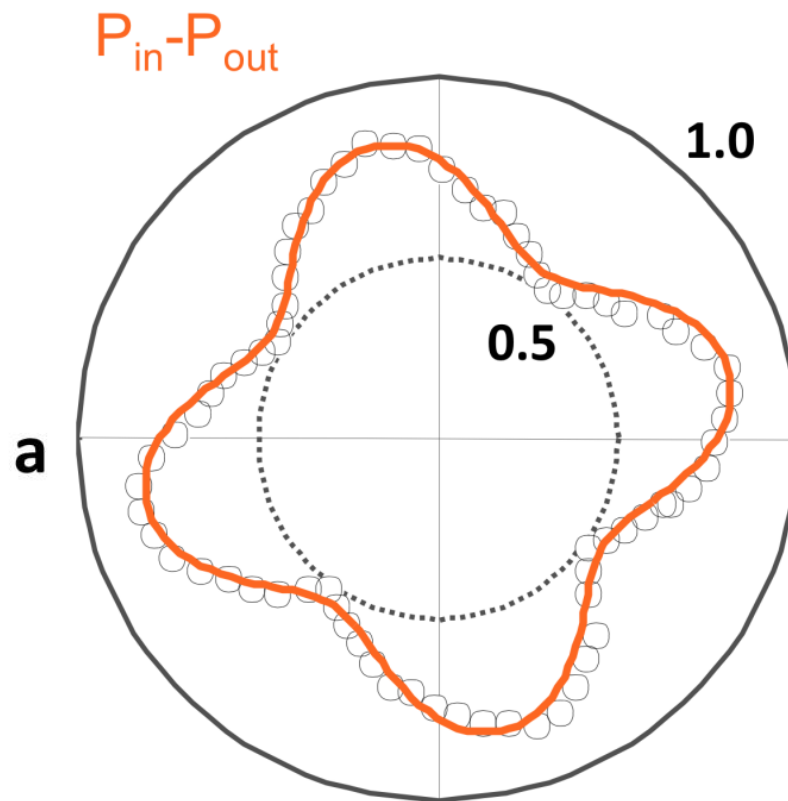
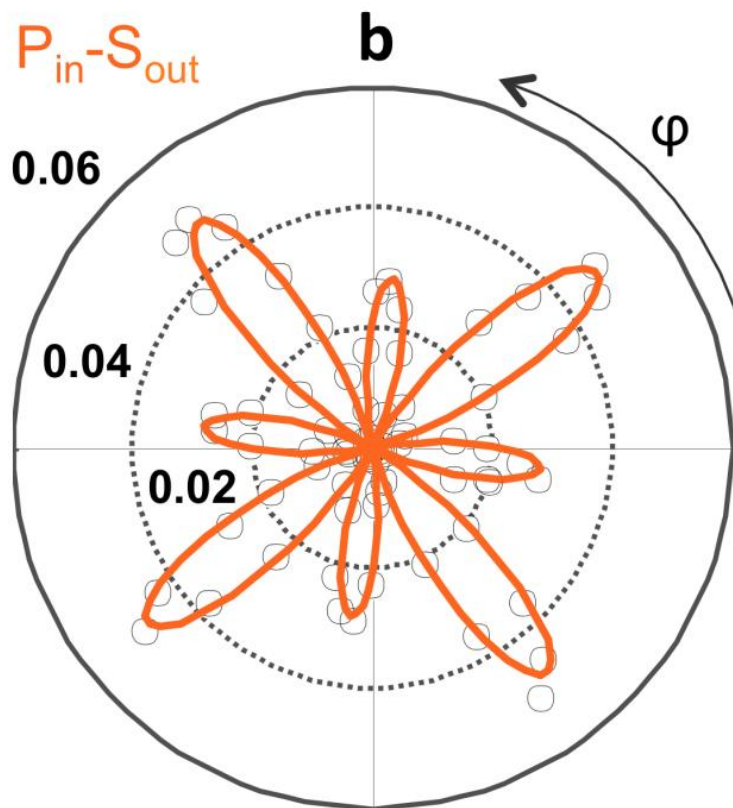


Consequences of lowered global symmetry

D. H. Torchinsky et al. PRL 114, 096404 (2015)

$$H = \sum_{n,n'} J \mathbf{S}_n \mathbf{S}_{n'} - D(S_n^x S_{n'}^y - S_n^y S_{n'}^x) \\ + \delta J_z S_n^z S_{n'}^z + \delta J_{xy} (\mathbf{S}_n \cdot \mathbf{r}_{n,n'}) (\mathbf{S}_{n'} \cdot \mathbf{r}_{n,n'})$$





$\chi^{EQ} E \nabla E$

 cryst. $4/m (C_{4h})$

Inversion sym.



Rotational sym.

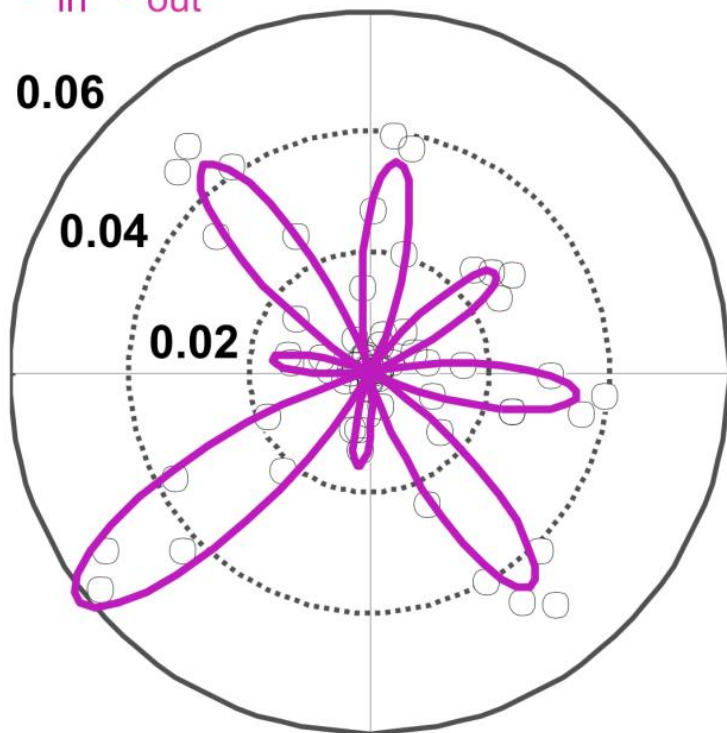
C_4

$P_{in} - S_{out}$

0.06

0.04

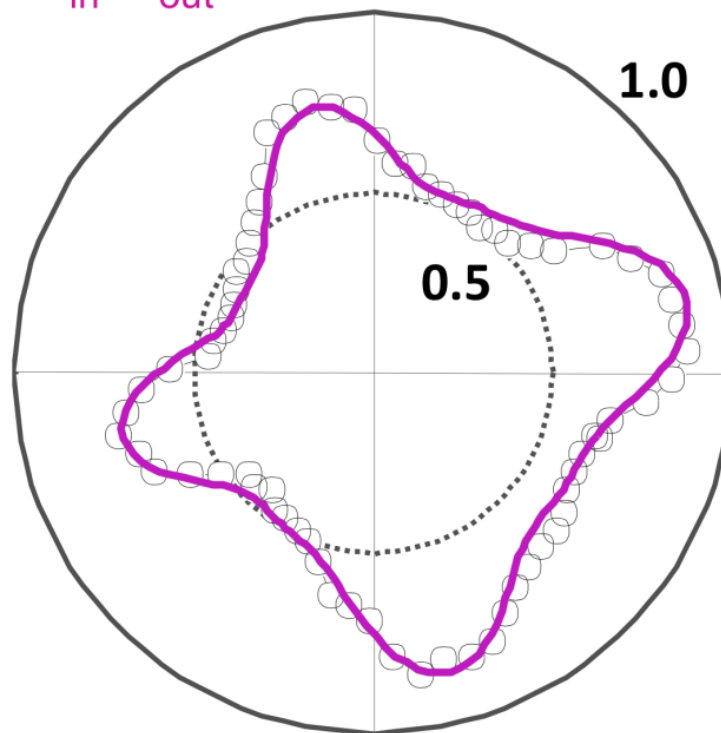
0.02



$P_{in} - P_{out}$

1.0

0.5



$$\chi^{EQ} \mathbf{E} \nabla \mathbf{E} + \chi^{ED} \mathbf{E} \mathbf{E}$$

cryst. $4/m$ magn. $2'/m (m1')$

Inversion sym.



Rotational sym.

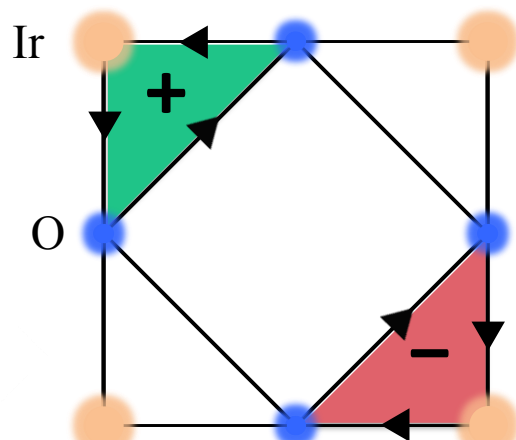
C_1

Symmetries of Θ_{II} loop current order (magneto-electric)

Properties: C_4

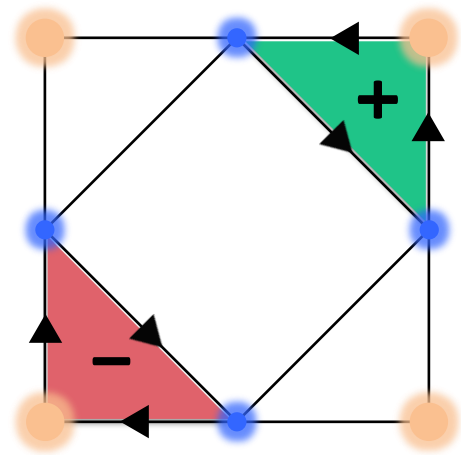
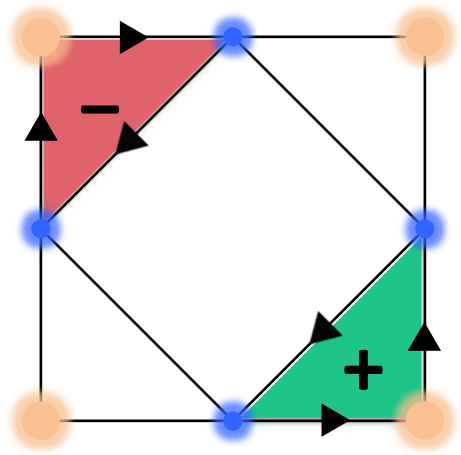
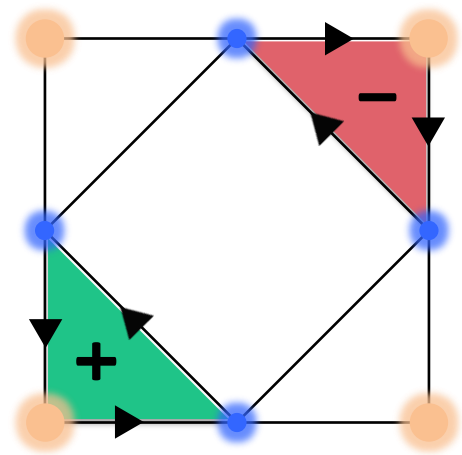
- $Q = 0$;
- **No Net Magnetization per unit cell;**
- **Non-Dipolar;**
- **Domain Average.**

C_1 & Broken Inv. & T. R.



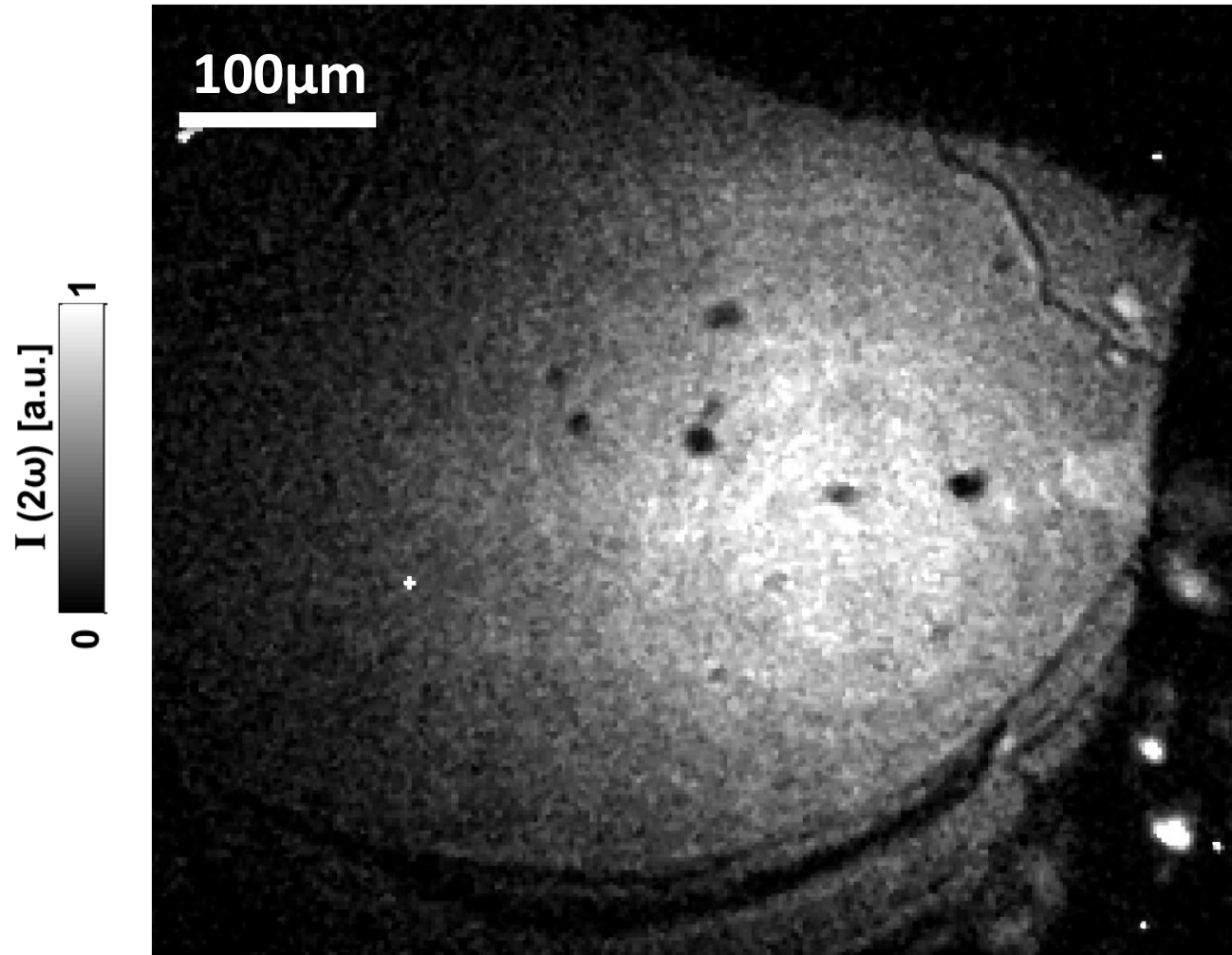
Ref:

C. M. Varma PRB, **55**, 14554 (1997)
C. M. Varma PRL, **83**, 3538 (1999)
C. M. Varma PRB, **73**, 155113 (2006)
C. Weber *et al.* PRL, **102**, 017005 (2009)
Y. F. Kung *et al.* PRB, **90**, 224507 (2014)
J. Orenstein PRL, **107**, 067002 (2011)
V. Yakovenko Physica B, **460**, 159 (2015)



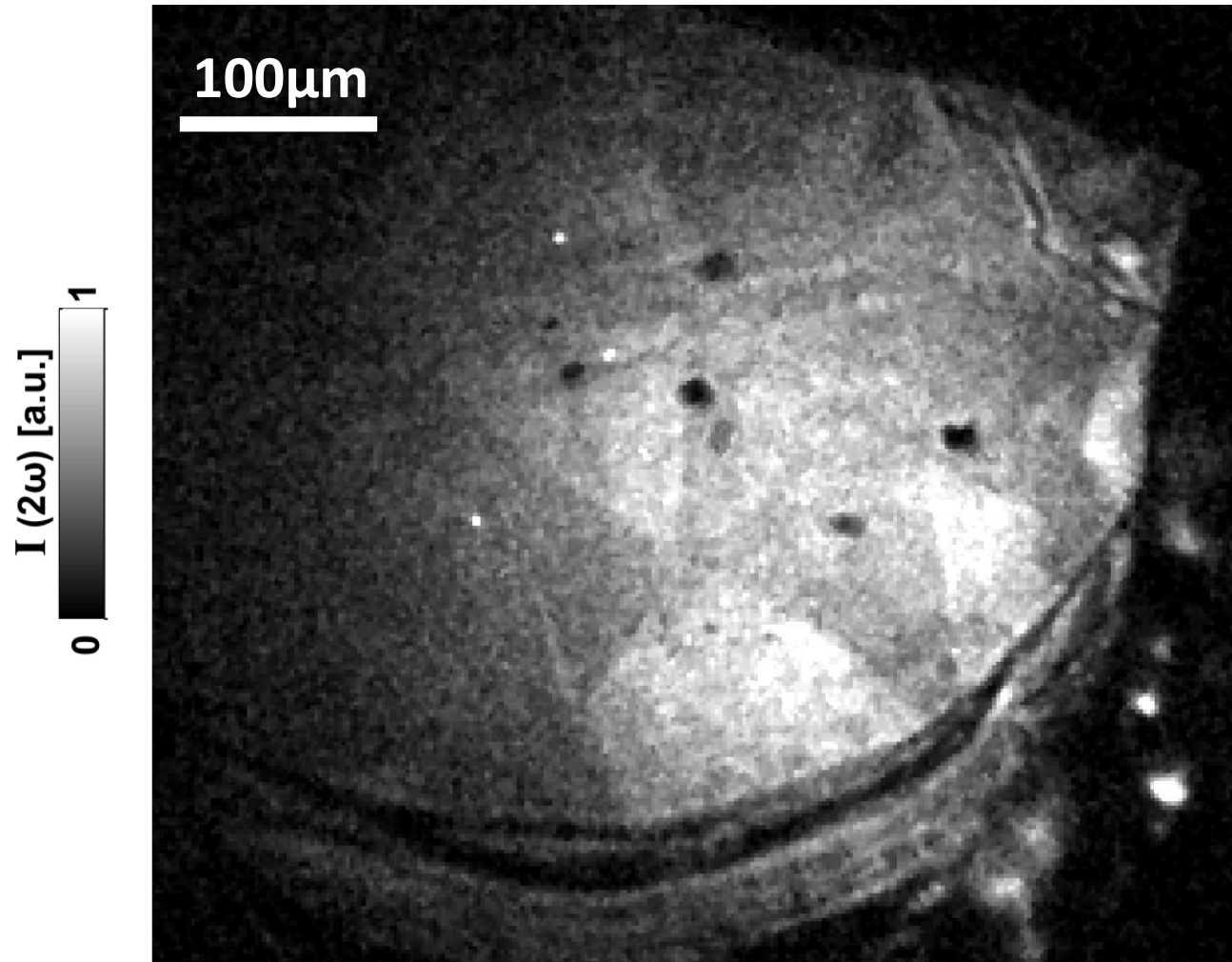
Nonlinear optical microscopy images

$T = 295 \text{ K}$

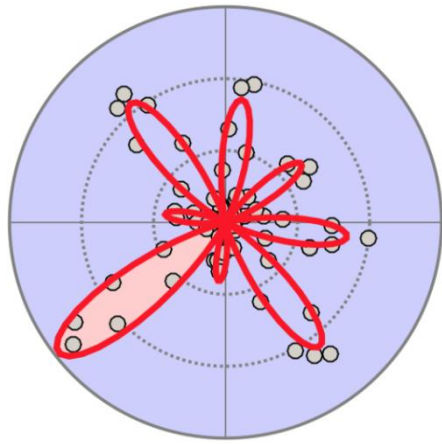


Nonlinear optical microscopy images

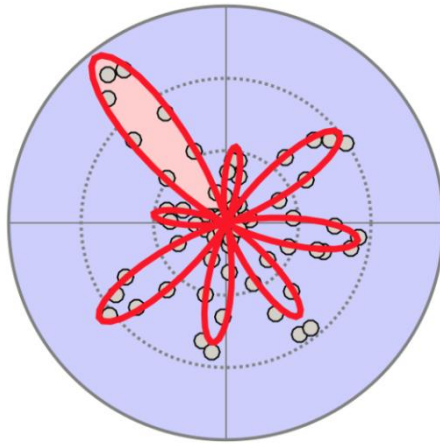
$T = 175 \text{ K}$



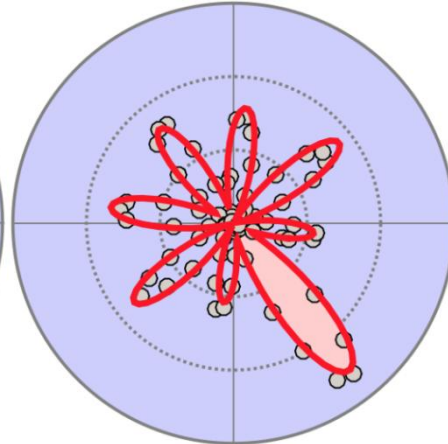
Hidden order domain orientations in Sr_2IrO_4



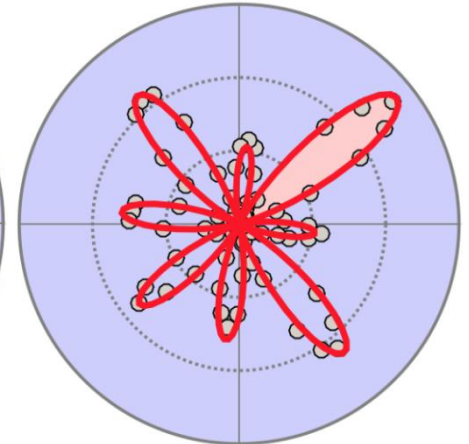
Domain I



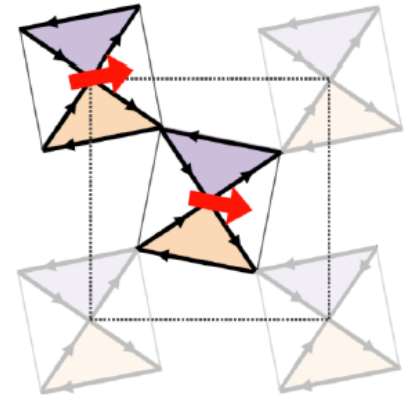
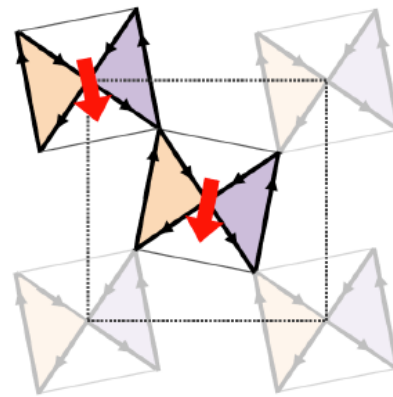
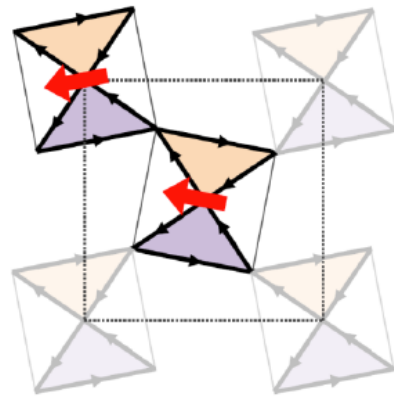
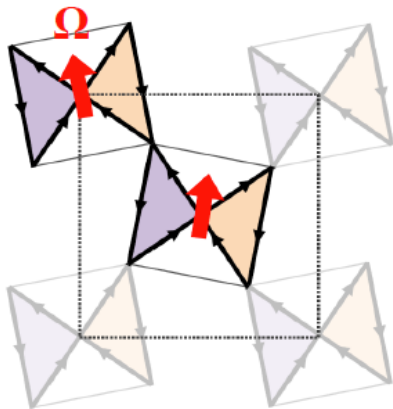
Domain II



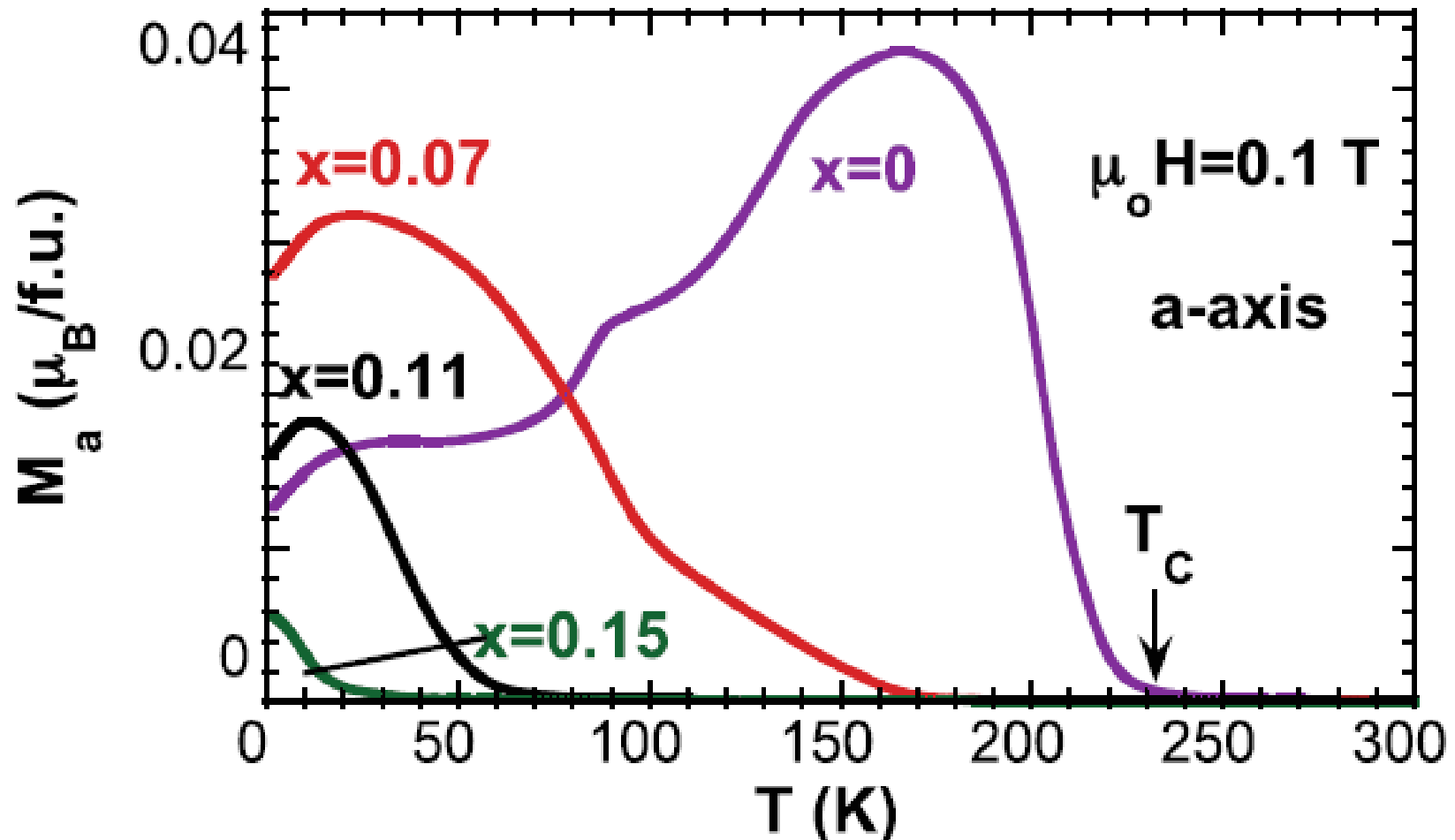
Domain III



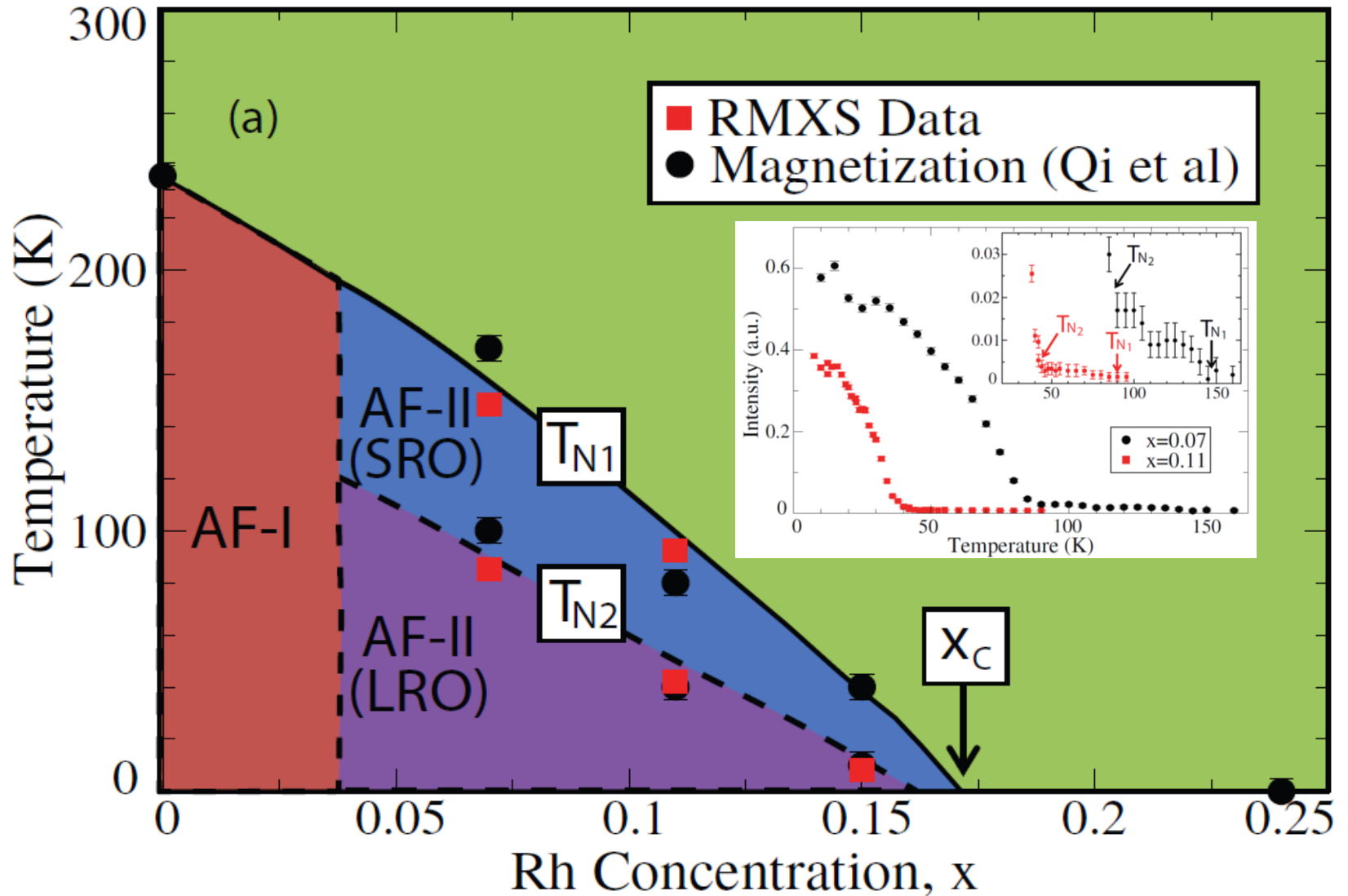
Domain IV



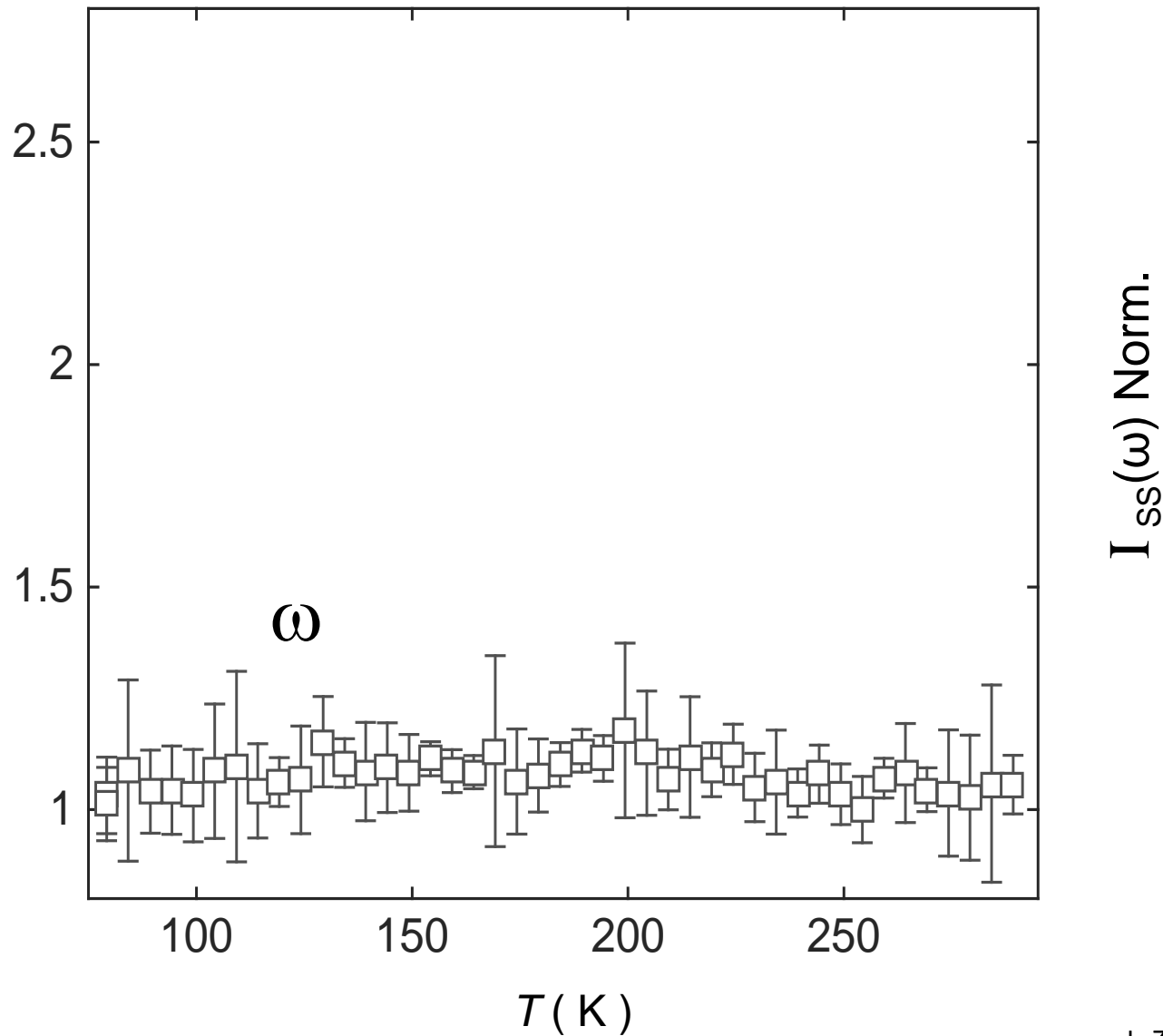
Hole doped $\text{Sr}_2\text{Ir}_{1-x}\text{Rh}_x\text{O}_4$



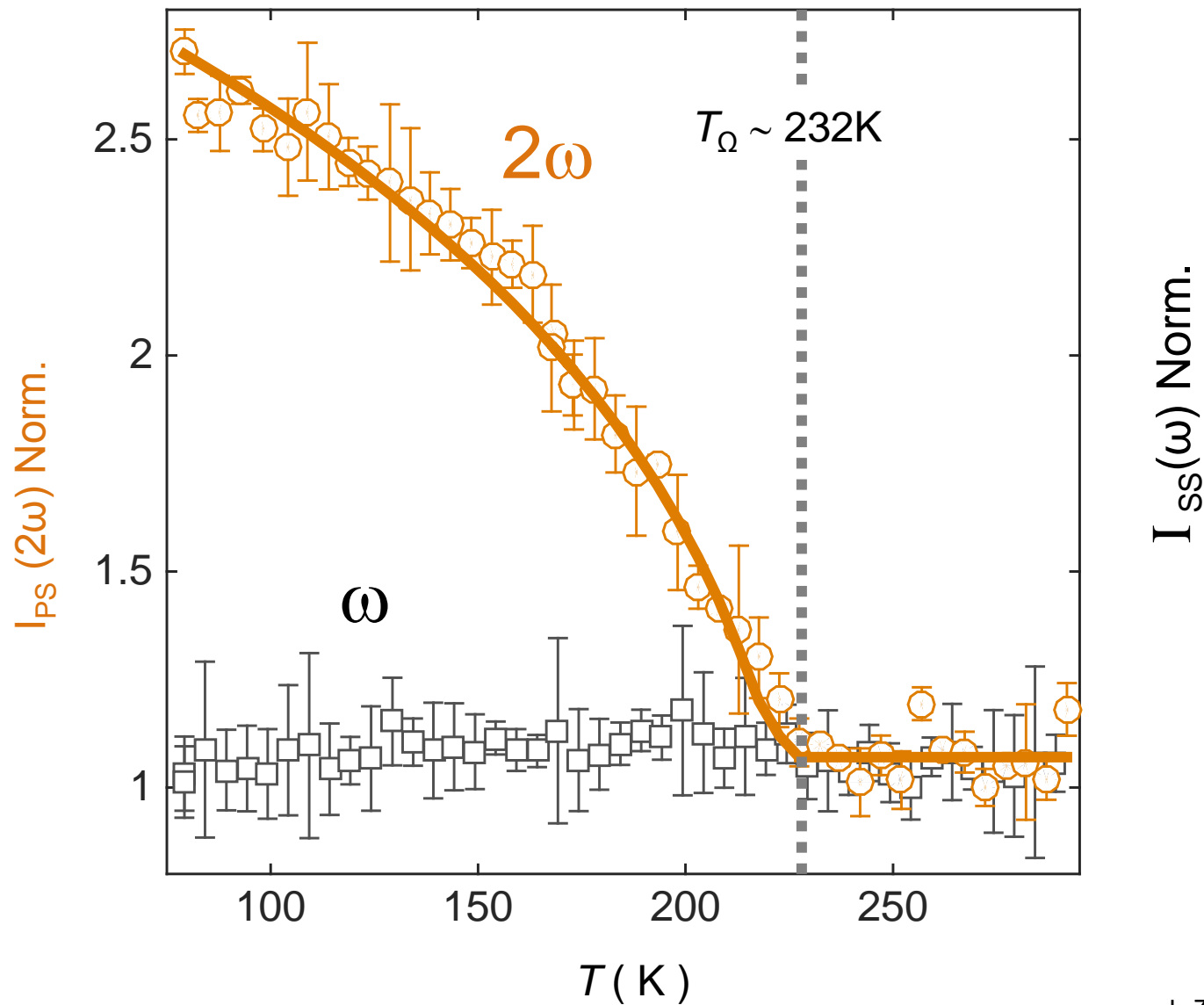
Hole doped $\text{Sr}_2\text{Ir}_{1-x}\text{Rh}_x\text{O}_4$



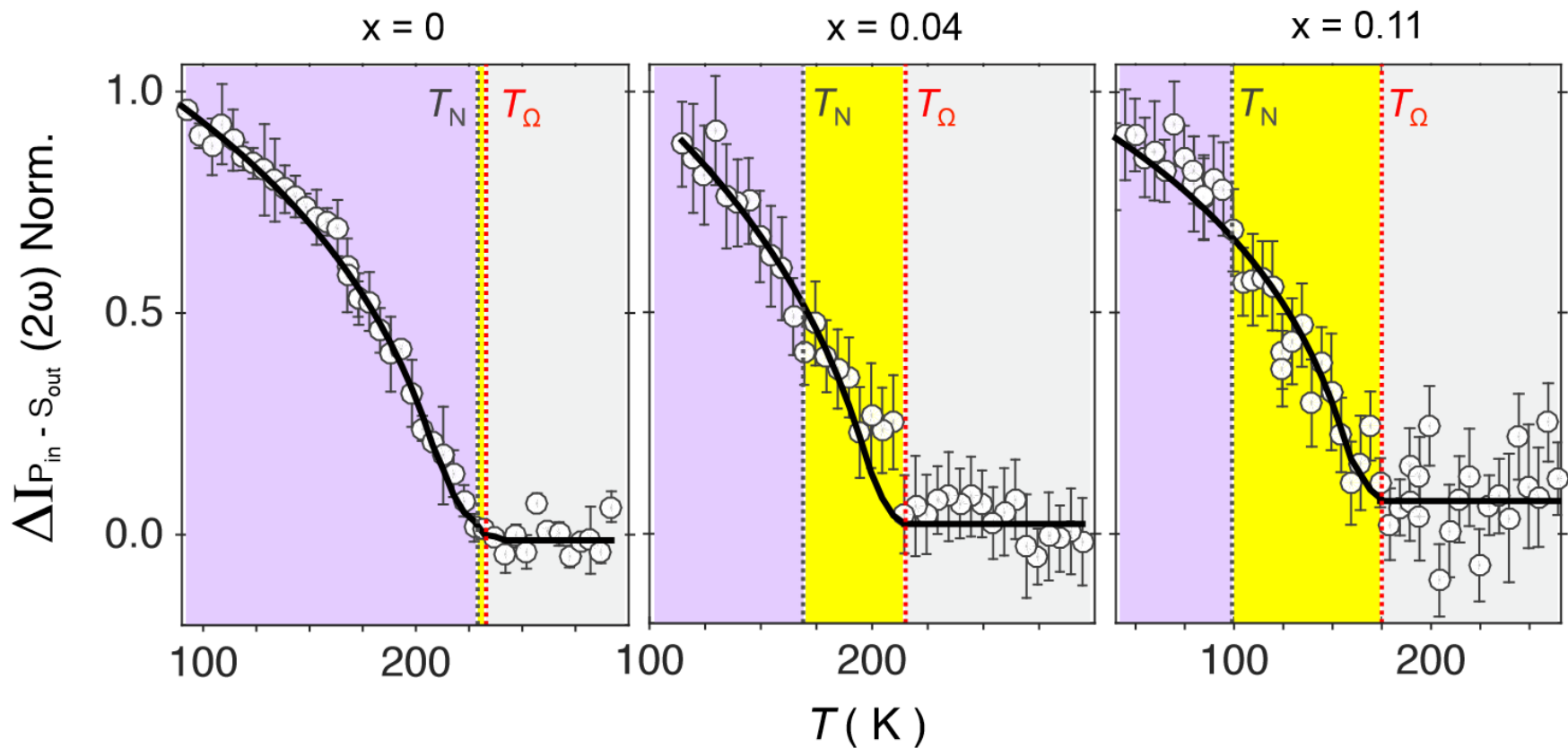
Hidden symmetry breaking below T_{Ω}



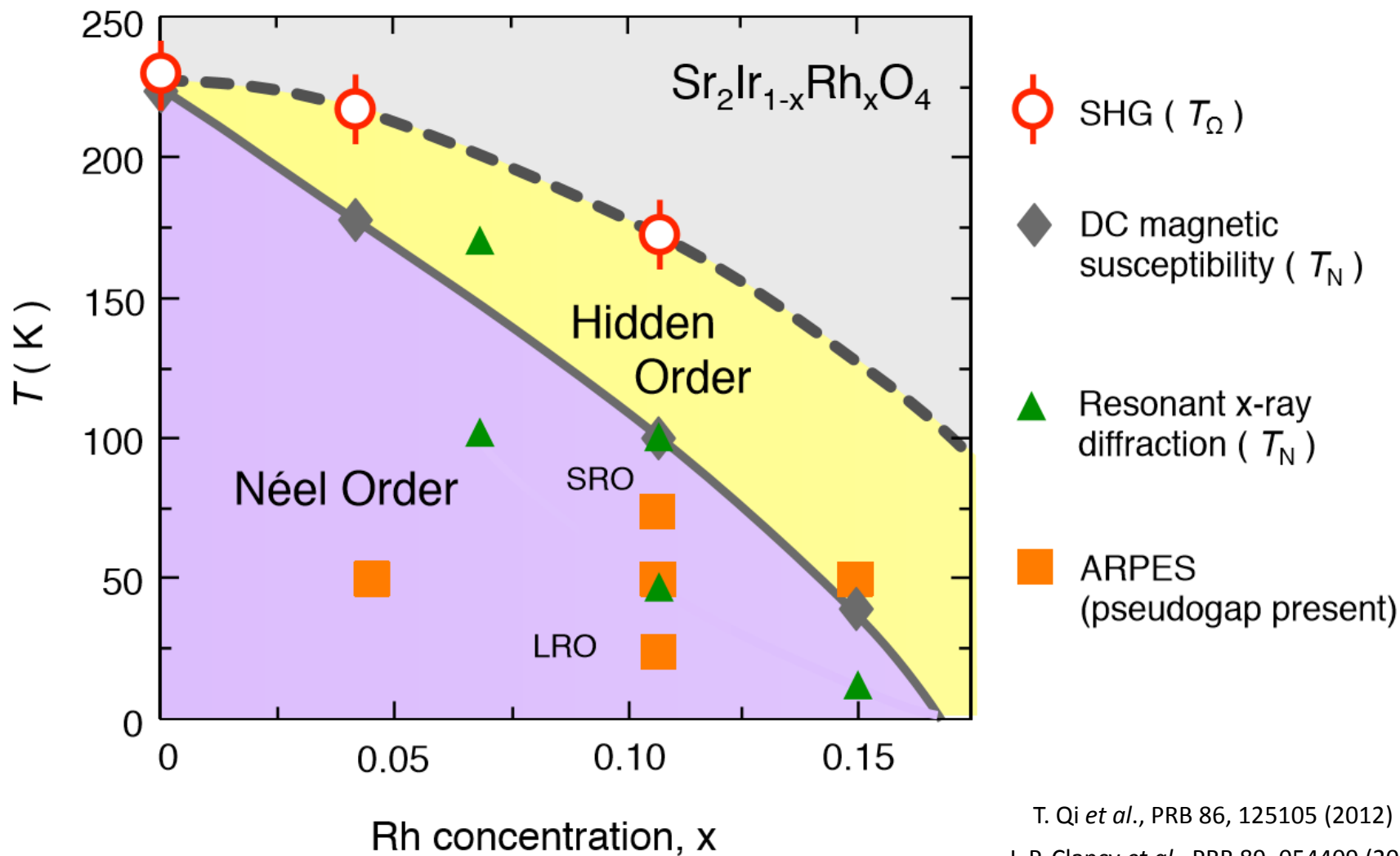
Hidden symmetry breaking below T_{Ω}



Doping dependence of T_Ω in $\text{Sr}_2\text{Ir}_{1-x}\text{Rh}_x\text{O}_4$



Exotic phases in iridates?



T. Qi *et al.*, PRB 86, 125105 (2012)

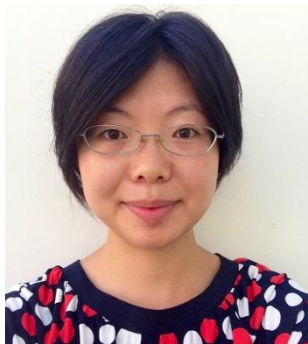
J. P. Clancy *et al.*, PRB 89, 054409 (2014)

Y. Cao *et al.*, <http://arxiv.org/abs/1406.4978> (2014)

Conclusions and Outlook

- Nonlinear optical response is an effective probe of bulk structural and electronic symmetry breaking.
- Complementary to neutron and (non-) resonant x-ray diffraction. Small crystals ✓ Spatial resolution ✓ Multipolar order parameters ✓ Strong neutron absorbers (e.g. Ir) ✓
- Lower global structural symmetry revealed in Sr_2IrO_4 . Supports perfect magneto-elastic locking.
- Hidden parity-odd magnetic phase revealed in parent and doped Sr_2IrO_4 consistent with Θ_{II} loop-current symmetry. Not trivially tied to Neel order.
- Possible relationship to pseudogap temperature?

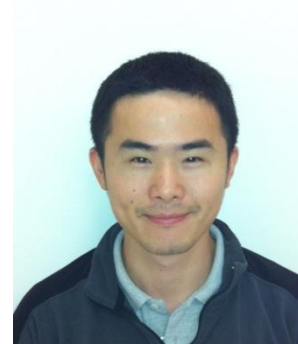
Acknowledgements



Dr. Liuyan Zhao



Dr. Darius Torchinsky



Hao Chu



Prof. Natalia Perkins
Dr. Yuriy Sizyuk



Prof. Gang Cao
Tongfei Qi



Prof. Rebecca Flint



Prof. Ron Lifshitz

Caltech

IQIM

